Carbon 196 (2022) 29–48

Contents lists available at ScienceDirect

Carbon

journal homepage: www.elsevier.com/locate/carbon

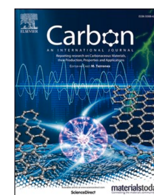

Polishing of polycrystalline diamond using synergies between chemical and mechanical inputs: A review of mechanisms and processes

Chen Xiao [a,b], Feng-Chun Hsia [a,b], Alexander Sutton-Cook [a,c], Bart Weber [a,b], Steve Franklin [a,d,e,*]

[a] Advanced Research Center for Nanolithography (ARCNL), Science Park 106, 1098XG, Amsterdam, the Netherlands
[b] Van der Waals-Zeeman Institute, Institute of Physics, University of Amsterdam, Science Park 904, 1098XH, Amsterdam, the Netherlands
[c] School of Chemistry, University of East Anglia, Norwich, Norfolk, NR47TJ, UK
[d] Department of Materials Science & Engineering, The University of Sheffield, Sheffield, S13JD, UK
[e] Department of Mechanical Engineering, The University of Sheffield, Sheffield, S13JD, UK

ARTICLE INFO

Keywords:
Chemical mechanical polishing
Polycrystalline diamond
Material removal rate
Surface roughness
Oxidation
Mechanochemistry

ABSTRACT

Polycrystalline diamond (PCD) deposited as a thin film is an attractive material, both technologically and from a scientific viewpoint, due to its unique combination of properties. However, because many applications require the PCD to have a high quality surface finish, efficient and cost-effective polishing has become a critical and limiting step in advancing the more widespread use of PCD. The most widely-used processes for the polishing of PCD make use of synergies that can be achieved through applying a combination of chemical and mechanical inputs. This paper reviews the current state-of-the-art of such processes, which are mainly represented by chemical mechanical polishing (CMP) technology, for the polishing of PCD. An in-depth and informative literature survey is presented of the effects of the PCD characteristics and process-dependent factors such as polishing slurry composition, polishing pad/plate material, and polishing parameters, on the polishing/material removal rate and surface quality. Particular attention is given to the underlying mechanisms governing the material removal during polishing, which are complex and vary depending on the process, and are still unclear. Three main routes to material removal during the polishing of diamond are identified and summarized based on experimental results, chemical characterizations and computational simulations: interfacial mechanochemical removal, chemically-stimulated mechanical removal, and mechanochemical transformation of diamond. Finally, more recently developed polishing methods that make use of ultraviolet and plasma irradiations are introduced, and the limitations of existing research and future research directions are discussed.

1. Introduction

Diamond is an allotrope of carbon. Its unique natural face-centered cubic crystal structure (Fig. 1a) makes it attractive both technologically and from a scientific viewpoint due to its extraordinary combination of properties [1–5]: 1. It has the highest hardness/bulk modulus of any material found in nature, with micro hardness up to 10000 kg/mm^2, making it an excellent material for long-lasting micromechanical parts and machining tools [6–11]; 2. It has extremely high thermal conductivity (up to 22 W/(cm·K)), which makes it an ideal heat dissipation material for electronic devices [12,13]; 3. Diamond offers very high light transmittance for anti-corrosion and wear-resistant infrared optical windows and high-power laser windows [14]; 4. The diamond band-gap, up to 5.5 eV, is ideal for the fabrication of high reliability semiconductor devices [15,16]; 5. Strong chemical stability, corrosion resistance and radiation resistance makes diamond suitable for applications in harsh environments [17–19]; 6. The nitrogen-vacancy center point defect in diamond allows photoluminescence properties that can be utilized, for example, in quantum computing. However, due to the scarcity of diamond in nature and its high price, the demand for lab grown crystalline diamonds with regular shape and different grain sizes has aroused research interest with a large number of scholars. In 1962, Eversole pioneered in producing diamond by chemical vapour deposition (CVD) [20]. Diamond synthesis developed rapidly in the following

Abbreviations: PCD, Polycrystalline diamond; CMP, Chemical Mechanical Polishing; MRR, Material Removal Rate.

* Corresponding author. Advanced Research Center for Nanolithography (ARCNL), Science Park 106, 1098XG, Amsterdam, the Netherlands.
E-mail address: s.franklin@arcnl.nl (S. Franklin).

https://doi.org/10.1016/j.carbon.2022.04.028
Received 4 February 2022; Received in revised form 4 April 2022; Accepted 11 April 2022
Available online 19 April 2022
0008-6223/© 2022 The Authors. Published by Elsevier Ltd. This is an open access article under the CC BY license (http://creativecommons.org/licenses/by/4.0/).

decades to achieve low-cost and large-scale production of lab grown diamonds. A variety of diamond film preparation methods have emerged, such as microwave plasma-enhanced CVD, radio-frequency CVD, hot filament CVD, flame CVD and laser CVD, etc. [21–24].

Although CVD diamond films have the same or similar intrinsic properties as natural diamond, the growth process tends to result in thickness asymmetry, randomly oriented crystals, heterogeneous grain structure, high internal stress and a rough surface. These deficiencies often seriously restrict the industrial application of synthetic diamond films. For example, when synthetic diamond is used as a super-hard coating on cutting tool surfaces, the surface roughness has a significant impact on the cutting efficiency, accuracy of the machined part and topography of the machined surface [25]. The surface roughness is also important in the application of diamond coatings as the heat dissipation material in integrated circuits and high-power components; the heat dissipation efficiency increases with increasing contact area, which is lower for rough coatings [12]. Furthermore, the transparency of optical diamond coatings is strongly reduced by absorption due to coating impurities and the scattering of light by the rough diamond surface [26]. Thus, polishing of diamond surfaces has become a necessary prerequisite to achieve the required excellent performance in various industrial applications and in daily life. The characteristics of high chemical inertness, superior mechanical properties, high wear resistance, strong anisotropy and heterogeneity of diamond make it extremely difficult to machine diamond films. Therefore, effectively polishing diamond films with low damage has become a key issue in order to expand CVD diamond applications.

This review aims to discuss the polishing of polycrystalline diamond (PCD) in which synergies between chemical and mechanical inputs are present, which is mainly represented by Chemical mechanical polishing (CMP) technology. In this review, the focus is on the material removal behaviors and mechanisms occurring during the polishing process. Some of the discussions on PCD surfaces are addressed using results from research on single crystal diamond (SCD), for which the mechanisms have been studied to a greater extent, especially in computational simulations where SCD is commonly used to model and elucidate the interfacial reaction processes and mechanisms. Some advanced polishing methods that have not yet been applied to PCD but which are promising for the near future and do not conflict with polishing principles, are included in this review in order to give a more comprehensive understanding of the current status of diamond polishing research and to inspire future research directions.

1.1. Classification of PCD films

Conventionally, diamond coatings are classified according to average grain size as microcrystalline diamond (MCD, > 100 nm), nanocrystalline diamond (NCD, 10–100 nm) and ultrananocrystalline diamond (UNCD, < 10 nm), see Fig. 1b [27,28]. Prior to deposition, a surface to be coated needs to be pre-treated by "seeding" nano or micro diamond particles on the substrate surface. This is necessary to enable and improve the subsequent diamond nucleation. After seeding, the diamond growth process involves a hydrogen-rich chemical reaction for which CH_4 and H_2 gases are supplied to the chamber. Generally, MCD is produced using very low CH_4 percentages (<2%) and NCD with 1–10% CH_4 (depending on seeding density, desired film thickness, CVD method, reactor pressure, etc.) [29,30]. The columnar microstructure of MCD coarsens as the film grows, resulting in a highly faceted morphology with a root mean square (RMS) roughness that is usually about 10% of the film thickness. However, when nanoparticles are seeded using a very high nucleation density, NCD films with a smoother and higher quality surface compared to MCD can be produced under optimized deposition conditions [2,31,32]. In contrast to the hydrogen-rich growth environment used in the NCD case, UNCD films are generally grown in hydrogen-poor and argon-rich environments [30]. Extremely smooth surfaces with a RMS roughness of approximately 5 nm can thus be achieved. Carbon dimers (C_2), which have a low activation energy (~6 kcal/mol) for incorporation into the growing UNCD film, are thought to have a significant impact on the nucleation and growth process [2]. Compared to MCD and NCD, the surface roughness of UNCD is less dependent on the film thickness, which makes it possible to obtain ultra-smooth UNCD films that are sufficiently thick. The nanocrystalline grains (2–5 nm) on UNCD films are surrounded by grain boundaries consisting of carbon that is not in diamond form [33]. For this reason the corrosion resistance of UNCD, with a higher sp^2-bonded carbon component (up to 5%), is less than that of MCD with its high sp^3 bonding character and NCD, which in high quality films has <0.1% sp^2 [30]. This means that electrochemical corrosion problems can occur when UNCD coatings are used in environments such as sea water. The microstructure of PCD has a strong effect on mechanical properties such as strength, toughness, and flaw size distribution [34]. The grain boundaries in diamond thin films are typically weaker than the grain facets, thus the reduction of grain size increases the grain boundary area and reduces the fracture toughness [35].

1.2. Basic knowledge of diamond polishing

Polishing of diamond has a decades-long history and was initially dominated by mechanical and chemical polishing processes. Due to its ultra-high hardness and chemical inertness, it is difficult to polish the diamond substrate satisfactorily using purely mechanical or chemical inputs: purely mechanical polishing (MP) can result in severe

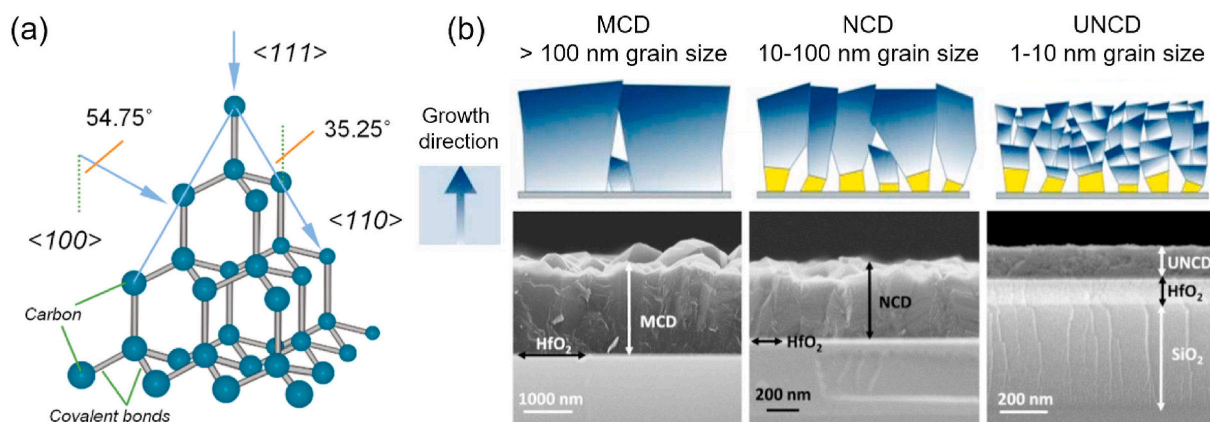

Fig. 1. (a) Schematic structure of single crystalline diamond. (b) Diagrammatic presentation and scanning electron microscope (SEM) images of the cross-sectional view of different diamond phases (MCD, NCD, UNCD) deposited on Si substrates (Reproduced with permission [36]. Copyright 2016, Elsevier). (A colour version of this figure can be viewed online.)

subsurface/surface damage, whereas purely chemical polishing processes generally give a low polishing rate and poor surface consistency [37]. These disadvantages can be avoided by using synergies between chemical and mechanical interactions in diamond polishing. CMP is one of the most widely used surface finishing technologies for ultra large-area global planarization and is used for the surface planarization of integrated circuit chips, computer hard disks, micro mechanical systems, optical glass, etc. [38–41] However, traditional CMP technology has several shortcomings, especially in relation to polishing efficiency, environmental friendliness and processing costs. For this reason, many new processing methods that also make use of synergies between chemical and mechanical inputs are now under development, such as dynamic friction polishing (DFP), ultraviolet irradiation assisted polishing (UVAP), and plasma assisted polishing (PAP). The ultimate goals of PCD polishing with respect to most applications for diamond substrate components, which have been widely used in high-tech fields, should be similar to those of silicon substrates in integrated circuit applications. This would mean nm-level global geometric accuracy and sub-nm level roughness, while avoiding surface and subsurface damage. In addition, the ultimate goal for the material removal rate (MRR) should be to make it as high as possible, for example hundreds of μm/h is achievable using laser polishing, which provides the highest MRR in PCD polishing but poor surface quality [41].

Performing CMP on a diamond surface was first introduced by Thornton and Wilks in 1975 [42], and was further developed over the successive decades to obtain precision diamond surfaces. Since the rapid development of CVD technology in the 1980s, the CMP method has been successfully applied in the precision machining of CVD diamond films with a polishing rate (Fig. 2a) and surface quality (Fig. 2b–d) higher than pure MP. In a typical CMP process, shown schematically in Fig. 3a, the diamond sample is held in a rotating carrier against an elastic polishing pad where the wafer/carrier and the pad rotate in the same direction. The diamond surface undergoes a chemical reaction and the reaction products are continuously removed and taken away by the polishing slurry, which contains nanoparticle abrasives and oxidants and is continuously replenished. The combination of the grinding action of the nanoparticles and the corrosive action of the oxidants creates a high-precision surface on the work piece [43], enabling global planarization with a sub-micrometer feature size. As yet, the mechanisms of CMP are not fully understood from a microscopic point of view. From a macro perspective, CMP involves a combination of chemical corrosion and mechanical grinding. Heat generated by the friction between the abrasive particles and the polishing surfaces provides additional energy for the solid-phase chemical reactions. Chemicals in the polishing slurry react with the surfaces of the work piece, converting the high hardness, chemically stable diamond into softer and easier-to-remove structures. Due to the relative motion of the diamond sample to be polished and the polishing pad, abrasive particles in the polishing slurry grind the reaction layer on the work piece, removing this reaction layer to produce an ultra-smooth surface. Key indicators to evaluate the efficiency and quality of the CMP process are MRR, surface roughness, and subsurface/surface damage. As illustrated in Fig. 3b, the process control is very complex. The major factors of influence include equipment components (e.g. carrier, conditioner, and polishing pad), polishing parameters (e.g. downforce, speed, and reciprocating motion) and consumables (e.g. slurry). The final processing results (MRR and polishing quality) are governed by the synergistic action of all the processing factors.

Tsai et al. [44], found that the diamond film surface undergoes two stages within a 5-h polishing period. In the first stage, the authors established that some apexes of the crystals were removed, and observed many grooves and nicks on the polished diamond surface; however, the original rough shape of the diamond crystals remained. In the second stage, after approximately 1 h of the CMP process, the roughness value reduced sharply from ~800 nm to ~300 nm with corrosion reaction products covering the entire diamond surface. After 5 h of polishing, the roughness had further decreased to 95 nm and the roughness of some local areas on diamond crystal facets was estimated using atomic force

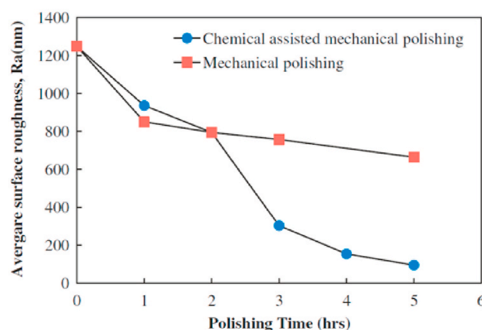

(a) Average roughness versus polishing time

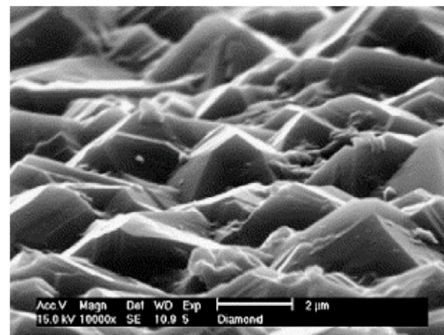

(b) Before polishing

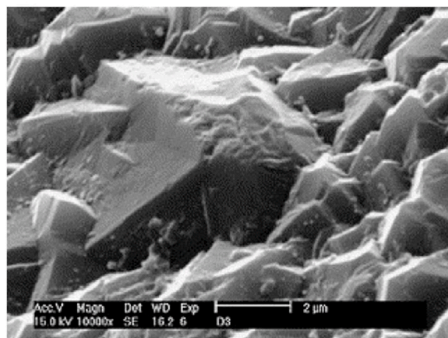

(c) Mechanically polished MCD surface

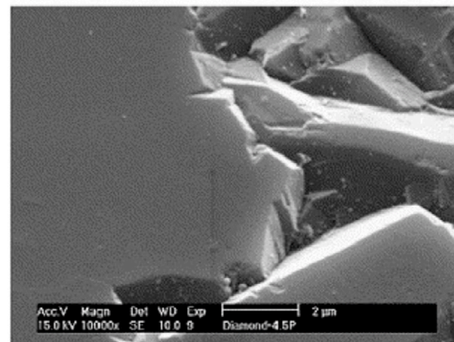

(d) Chemo-mechanically polished MCD surface

Fig. 2. (a) The average roughness of the diamond film at different MP and CMP durations. SEM images of the diamond films before (b) and after MP (c) and CMP process (d) (Copied with permission [44]. Copyright 2007, Elsevier).

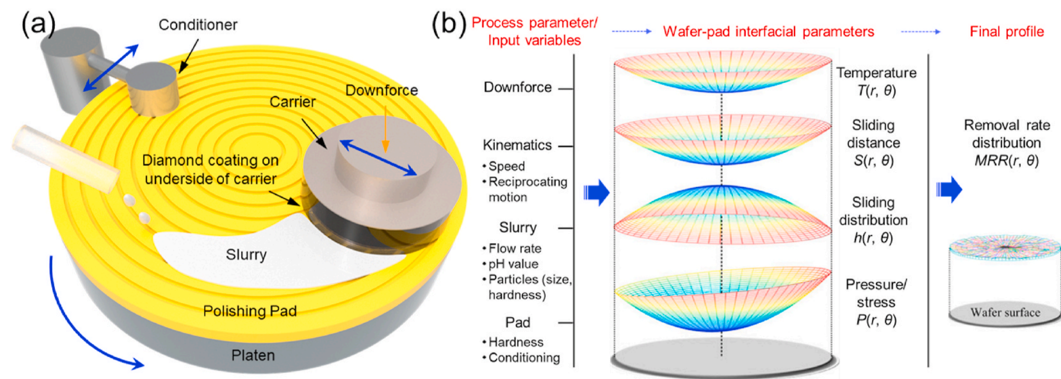

Fig. 3. (a) Schematic diagram of CMP. The diamond wafer is attached at the backside of carrier and polished. (b) CMP factors influencing the final polishing surface quality (Reproduced under the terms of the Creative Commons license [38]). (A colour version of this figure can be viewed online.)

microscopy (AFM) to be as low as 4.5 nm. However, cavities and cracks at crystal boundaries are obstacles to obtaining an entirely ultra-smooth surface with a roughness of Angstroms. Using appropriate CMP conditions, a low subsurface/surface damage diamond surface with an average roughness of 29 nm can be produced at an average MRR of 1.39 μm/h [45].

2. MRR and polished surface roughness

The MRR, sometimes termed polishing rate, together with the final roughness of the polished surface, are the most important performance indicators for diamond polishing procedures. As mentioned earlier (see Fig. 3), polishing processes for diamond involving a combination of both chemical and mechanical effects, exemplified by the CMP process, are very complex. The MRR is affected by many factors, leading to great challenges in process control and achieving a predictable outcome. In general, the factors of influence can be divided as follows: the intrinsic properties of the diamond film itself, the composition of the slurry, the polishing pad and the polishing parameters.

2.1. Effect of the intrinsic properties of diamond on the MRR

***Doping of diamond*:** Doping is one of the most common methods used to modify the intrinsic properties of PCD. Different doping elements and levels of doping have been shown to affect the MRR of diamond. For example, B and Si doping can improve the oxidation resistance (Fig. 4a), which reduces the mass loss of diamond in etching and CMP processes (Fig. 4b) [46]. However, when nitrogen is used as the doping element and incorporated within the doping source (N_2 or urea), the oxidation rate is increased, facilitating the CMP efficiency (Fig. 4) [46].

***Topography of diamond*:** The grain size of the diamond film affects the surface topography [47], and tribological behaviors [48–50]. The grain-size uniformity of PCD grown on Si wafer substrates has a strong influence on the resulting surface topography changes produced by CMP because any non-uniformity over the polishing surface leads to uneven interactions between the polishing pad and the slurry [51]. Starting from an already low as-deposited surface roughness, boron-doped UNCD can be polished to sub-nanometer roughness much more easily and cheaply than boron doped NCD or MCD. The individual diamond crystal orientation (e.g. <110>, <100> or <111>) has been shown to have lesser effect on the resulting surface topography in CMP using a SiO_2--based slurry [52], and on the MRR in CMP using a SiO_2 wheel in atmospheric conditions, compared with the mechanical lapping/polishing case (planarization by grinding using hard abrasive usually in the absence of a fluid environment) [53–55].

2.2. Effect of the polishing slurry on the change in surface roughness and MRR

In the CMP of PCD, polishing slurries can contain abrasives, including non-oxide and oxide abrasives, and oxidants to facilitate the diamond removal.

***Effect of the abrasive in the slurry*:** When diamond particles are included in the slurry, increasing the particle size has a large positive impact on the MRR (Fig. 5a) [56], but the final surface roughness of the PCD after polishing is greater compared to when smaller particles are used [45]. With oxide abrasives such as ceria (CeO_2), alumina (Al_2O_3), and silica (SiO_2) particles (Fig. 5b), increasing the particle size has a

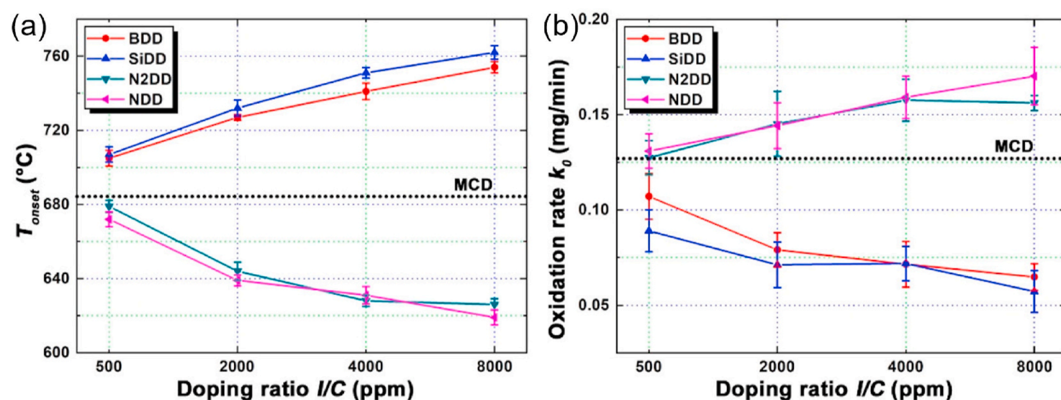

Fig. 4. (a) Oxidation rate of diamond coated samples as a function of doping ratio. (b) Mass loss as a function of time during CMP of diamond coated SiC samples. Boron-doped diamond (BDD), silicon-doped diamond (SiDD), nitrogen-doped diamond using N_2 as the doping source (N2DD), nitrogen-doped diamond using urea as the doping source (NDD) and MCD (Copied with permission [46]. Copyright 2020, American Chemical Society).

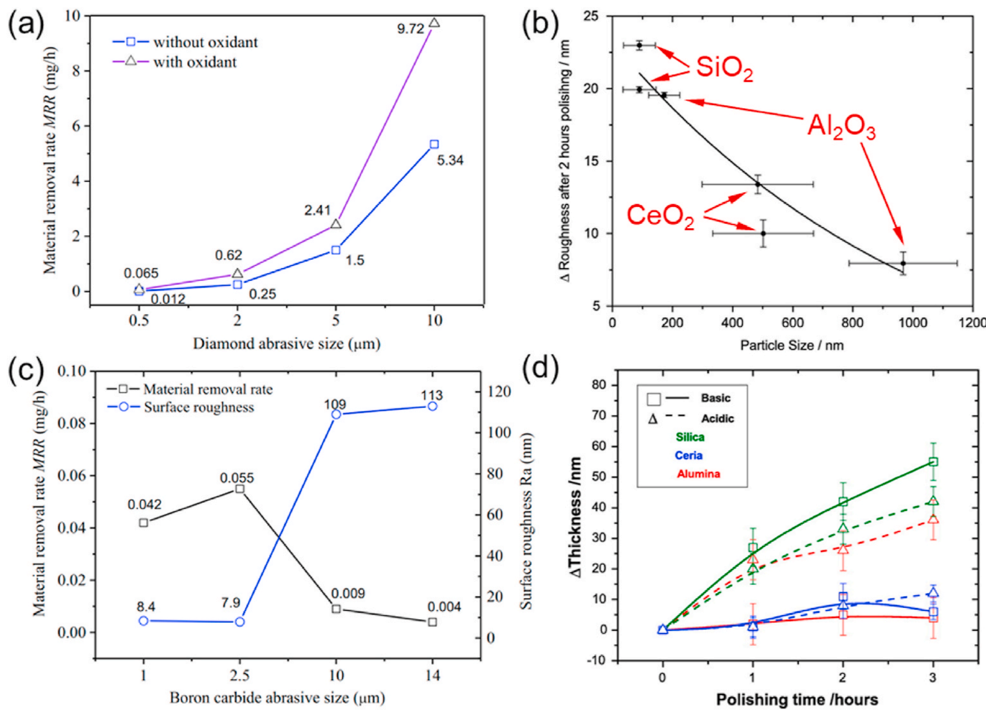

Fig. 5. The change in surface roughness or MRR of diamond samples in CMP as a function of particle size of (a) diamond abrasive (SCD) (Copied with permission [56]. Copyright 2018, Springer), (b) SiO_2, Al_2O_3, and CeO_2 abrasives (NCD) (Copied under the terms of the Creative Commons license [57]), and (c) B_4C abrasive (SCD) (Copied with permission [56]. Copyright 2018, Springer). (d) MRR of NCD surface (change in thickness after polishing, Δ thickness) as a function of polishing time by SiO_2, Al_2O_3, and CeO_2 abrasives (Copied under the terms of the Creative Commons license [57]). (A colour version of this figure can be viewed online.)

similar effect on the polished surface roughness, but the MRR is decreased rather than increased [57,58]. Boron carbide (B_4C), a non-oxide abrasive, shows a similar trend to the oxide abrasives: increasing abrasive particle size decreases the MRR but increases the final polished surface roughness (Fig. 5c). These observations are due to fundamental differences in the polishing mechanisms. Where chemical reactions dominate in the polishing process, as is the case with oxide and B_4C abrasives, the MRR is governed by the total contact area available for chemical interaction between the particles and the diamond film [56]. With increasing particle size, this total contact area A decreases ($A \propto C^{1/3}\phi^{-1/3}$, where C is the abrasive concentration in the polishing slurry and ϕ the particle size) [59], so a greater abrasive particle size reduces the MRR. In the case of diamond abrasive particles, the polishing process is dominated by mechanical rather than chemical interactions. Since mechanical interactions are governed by the indentation volume V, which increases with increasing abrasive particle size ($V \propto C^{-1/3}\phi^{4/3}$), a larger particle size gives, in the case of diamond particles, an increased MRR [59]. It has also been shown that adding an active metal such as Ti to Al_2O_3 abrasive promotes a chemical reaction between the Ti and diamond that lowers the activation energy for graphitization of the diamond. Since graphitized diamond is easier to remove through mechanical abrasion than the original diamond, this increases the MRR [60]. The type of oxide abrasive used in the polishing plays an important role in the MRR of NCD. Werrell et al. showed that, for both basic and acidic polishing solution, the MRR resulting from SiO_2 abrasive is much higher than when Al_2O_3 and CeO_2 are used (Fig. 5d) [57]. However, the mechanism for this difference remains unclear: the authors found that no single natural property (such as bond energy/dissociation energy (Ce–O (790 kJ/mol) > Al–O (502 kJ/mol) ≥ Si–O (452 kJ/mol)) [61], chemical activity (Ce–O > Si–O > Al–O), mechanical properties (hardness and mechanical properties), etc.) was able to explain the MRR results sufficiently. Clearly, more in-depth and systematic studies need to be conducted in order to elucidate the different magnitudes of the effects of different oxide abrasives.

Effect of non-abrasive slurry components (oxidizers, additives etc.) & **pH:** When performing CMP on diamond, increasing the oxidation of the diamond surface tends to result in a higher MRR and lower surface roughness (Figs. 5a and 6b). A polishing slurry with a greater oxidizing potential and/or a greater concentration of OH radical groups leads to a greater decrease in surface roughness [62–67]. There is much evidence to support this. For example, an increased MRR was found in the polishing of SCD when using slurries containing Fe^{2+}, in which the electron

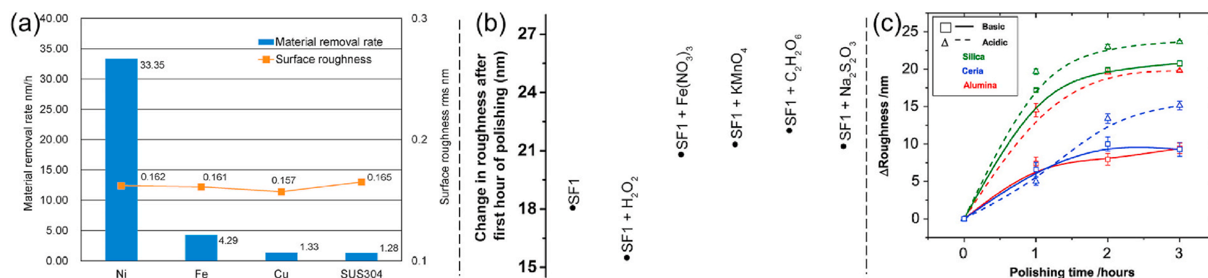

Fig. 6. (a) MRR and surface roughness of SCD samples by performing CMP on different types of metal plate in H_2O_2 solution: nickel (Ni), iron (Fe), copper (Cu) and 304 stainless steel (SUS304) (Copied with permission [65]. Copyright 2016, Elsevier). (b) The change in roughness of NCD films comparing pure alkaline colloidal silica slurry (SF1 slurry) with SF1 containing different oxidation agents: hydrogen peroxide (H_2O_2), ferric nitrate ($Fe(NO_3)_3$) and potassium permanganate ($KMnO_4$), and two reducing agents: oxalic acid ($C_2H_2O_4$), and sodium thiosulfate ($Na_2S_2O_3$) (Copied with permission [68]. Copyright 2018, Elsevier). (c) The decrease of RMS roughness of NCD films against CMP polishing time with basic or acidic slurries containing different types of abrasive particles (Copied under the terms of the Creative Commons license [57]). (A colour version of this figure can be viewed online.)

abundance of Fe^{2+} activates the carbon bonds of the diamond substrate [62,64]. In addition, when an Fe or Ni metal polishing plate is used in the CMP of SCD in the presence of H_2O_2 solution, the production of hydroxyl groups on the diamond surface by the H_2O_2 chemical oxidant also leads to an increase in MRR (Fig. 6a) [64,65]. In the polishing of polycrystalline NCD using an alkaline colloidal silica slurry containing different oxidation and reducing agents in an aqueous environment, the chemical action of these agents in the slurry was shown to give a greater change in roughness than that resulting from the silica alone (Fig. 6b) [58,63,68]. Furthermore, the change in roughness of NCD as a result of CMP is significantly affected by the pH of the aqueous environment, depending on the oxide abrasive used in the polishing slurry, with acidic environments giving the greatest effect (Fig. 6c) [57,63]. This is consistent with the MRR results shown in Fig. 5d.

2.3. Effects of polishing pad/plate on the MRR

Although much of the published work relating to the effect of polishing pad/plate on MRR was carried out on SCD, similar results may be expected for PCD. When both mechanical and chemical effects are present in the polishing process, the mechanical and material properties of the polishing pad can lead to different underlying polishing mechanisms. On the one hand, a greater hardness of the polishing pad, for example when metal or ceramic materials are used, leads to a greater MRR through micro-cracking as well as corrosion mechanisms [66]. On the other hand, if soft polyurethane/polyester pads are used for the CMP of diamond in combination with an oxidizing agent and oxide abrasive slurry, the MRR and surface roughness change is determined by the composition of the slurry rather than the qualities of the polishing pad [54,57,68,69]. When using an iron polishing pad without slurry in an ambient environment, the diamond removal process is dominated by the diffusion of carbon atoms from the diamond into the iron plate [64]. It has been reported that this diffusion of carbon atoms is inhibited when an H_2O_2 bath is used [70], but that, at least with SCD, the H_2O_2 bath leads to a lower surface roughness after CMP (Fig. 7) [64,70]. A comparison of diamond CMP using metal pads made of Fe, Cu, Ni, and SUS304, in slurry solution with an oxidation agent (H_2O_2) present, showed that, of the metals investigated, Ni produces the highest MRR (Fig. 6a) [65].

2.4. Effects of polishing parameters on the MRR

Effect on applied load and pressure: For a given average gap between the polishing plate and the rough diamond substrate, the real contact pressure increases logarithmically with the applied load [71]. In the polishing of PCD using mechanically-stimulated chemical reactions, which will be discussed in detail in Chapter 3.1, experiments have shown that the MRR and surface roughness increases with increasing polishing pressure up to a certain point, after which they decrease (Fig. 8a). When using an aqueous-based polishing slurry with an abrasive, increasing the applied load leads to an increase in the decomposition of H_2O and H_2O_2 and a more heavily deformed diamond surface. The ensuing stimulation of chemical reaction between the oxidants, –OH and –H, abrasives, and diamond, then leads to increased friction (not shown in Fig. 8b) and MRR as the contact pressure increases (Fig. 8b) [62,67,72]. The reduction of the MRR at higher pressures shown in Fig. 8a occurs because, at a certain point, the abrasive particles become hindered from entering the contact interface region between the PCD sample and the polishing disk, in this way inhibiting abrasive-induced chemical reaction [56]. Summarising, two effects compete with each

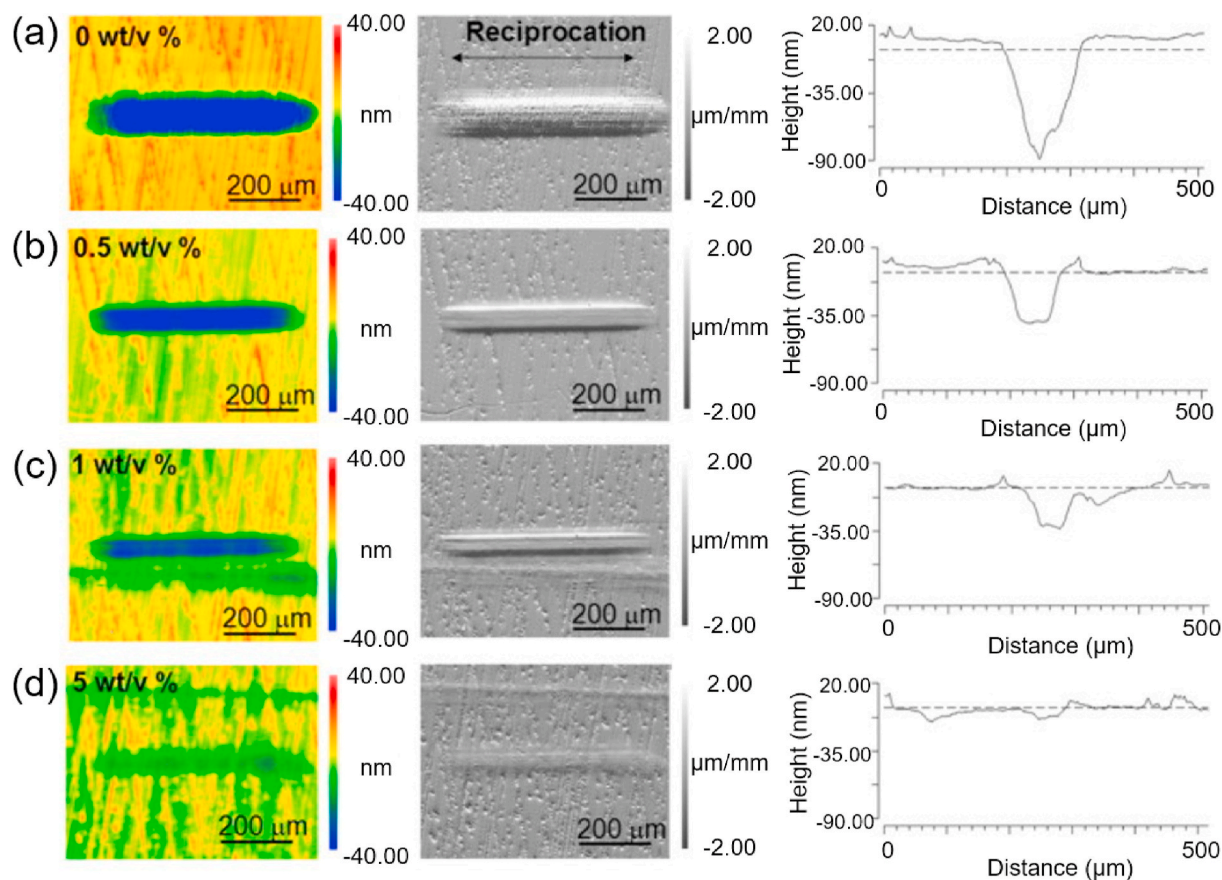

Fig. 7. Cross-sectional height profiles (right column) measured over the removal mark on SCD surfaces after polished in water (a) without H_2O_2 and with (b) 0.5%, (c) 1%, and (d) 5% H_2O_2 solution (Copied with permission [70]. Copyright 2016, Elsevier).

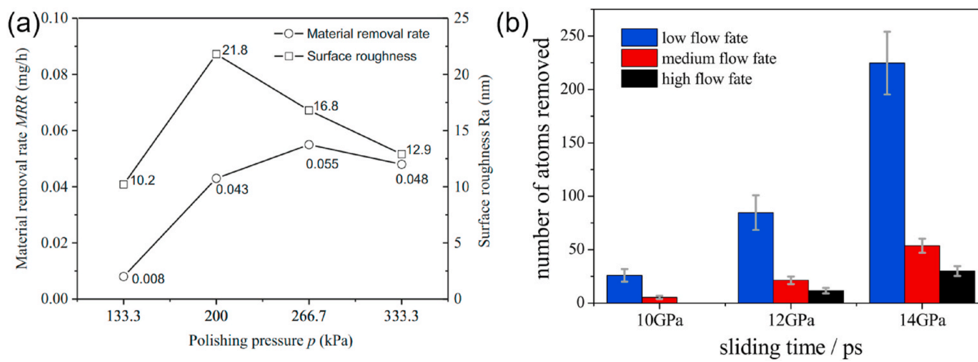

Fig. 8. (a) MRR and surface roughness of PCD by performing CMP under different polishing pressure (Copied with permission [56]. Copyright 2018, Springer). (b) Number of carbon atoms removed with respect to varying applied pressures and flow rates resulting from CMP using 10% H_2O_2 aqueous and diamond abrasive (calculated by Reactive force field molecular dynamics (ReaxFF MD) simulations) (Copied with permission [72]. Copyright 2020, Elsevier). (A colour version of this figure can be viewed online.)

other as the applied normal load increases: (1) decomposition of H_2O/H_2O_2 and deformation of the diamond surface, which increases the chemical reactivity, and; (2) hindering of the abrasive particles from entering the contact interface, which reduces the possibility of chemical interactions occurring. Which of the two effects dominates for a given normal load is likely to depend on a multitude of parameters including the size/shape, hardness and composition of the abrasive particles, flow rate, and other factors influencing the chemical reactivity.

Rotational/sliding speed of polishing pad: Modelling and experiments on the polishing of CVD diamond using a FeNiCr polishing pad show a positive correlation between rotation speed and interfacial temperature [71]. This correlation is also supported by experiments on the polishing of CVD diamond films using a borosilicate glass polishing pad with and without Ti (Fig. 9a) and a silica polishing pad (Fig. 9b) [53, 60]. In the case of CMP using an iron disk in 1% H_2O_2 solution, the MRR of SCD has been shown to increase linearly with rotational speed (Fig. 9c) [70]. ReaxFF MD simulations show that at the initial stage of diamond CMP in aqueous H_2O_2, increasing the sliding speed significantly increases the MRR at higher contact pressures (Fig. 9d), whereas the MRR is less dependent on the sliding speed at low contact pressures [73]. However, after a long sliding distance, the MRR shows stronger dependence on the sliding speed and is less dependent on the contact pressure [73]. The flow rate of the slurry also depends on the rotational speed of the polishing pad and ReaxFF MD simulations indicate that a high flow rate of an aqueous H_2O_2 slurry increases the passivation of diamond surfaces, which reduces the friction and wear behavior, thus lowering the MRR (Fig. 8b) [72].

Polishing temperature: In addition to external heating, a local increase in temperature during CMP may also be caused by friction generated between the CMP components (abrasive, pad/plate, diamond substrate) [63,66,71]. Increasing the temperature at the polishing interface of the CMP process results in an increased rate of chemical reaction of the diamond substrate, although if the temperature becomes too high this can also cause evaporation of the slurry as well as decomposition of the oxidant, for example K_2FeO_4 [63,66]. As a result, increasing temperature leads to an increase in MRR up to a certain point, after which a further increase in temperature gives a decrease in MRR (Fig. 10). This observation may be attributed to increased probabilities of the oxidation reactions of diamond at higher polishing temperatures [56]. When using a "soft" polishing pad, such as a polyurethane pad, an increase in the temperature decreases the hardness of the pad, which leads to an increased contact area between the pad and the diamond substrate and increased wear of the diamond [63]. When the temperature is greater than the melting point of the oxidants, this leads to enhanced chemical activation of the slurry components and/or an increase in the rate of reaction between oxidant and diamond substrate

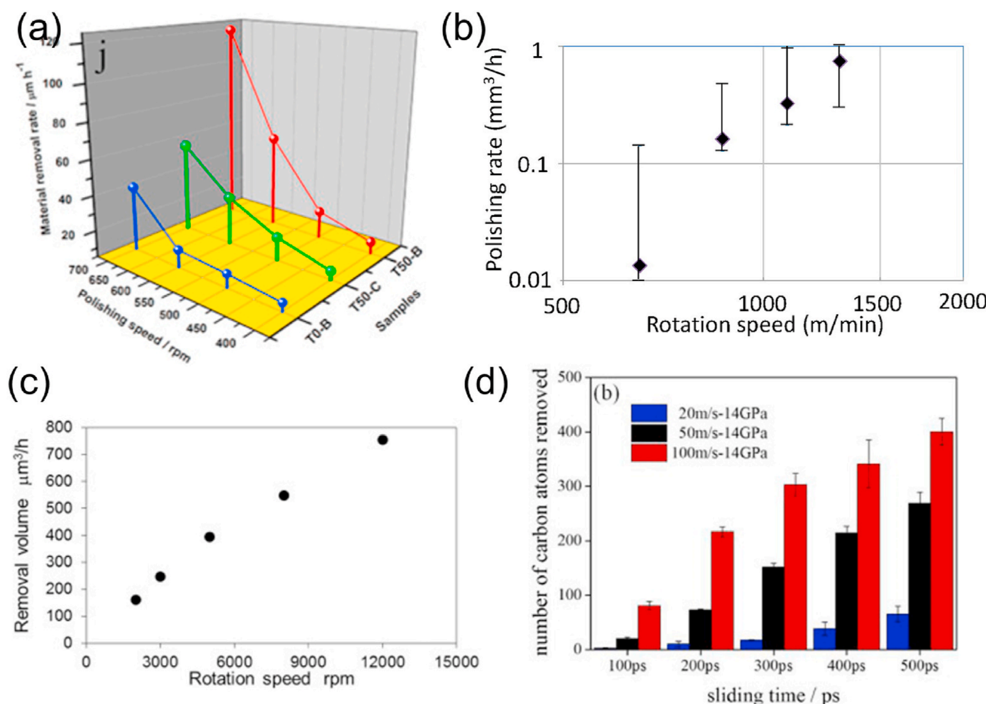

Fig. 9. (a) MRR as a function of polishing speed of MCD film after CMP process by using the composite polishing pad without Ti (T0-B), 50 wt% Ti (T50-B) and Cu–Sn+50 wt % Ti (T50-C) (Copied with permission [60]. Copyright 2018, Elsevier). (b) Polishing rate of SCD under various rotation speed of the SiO_2 polishing pad (Copied with permission [53]. Copyright 2016, Elsevier). (c) Removal volume of SCD linearly increases with rotation speed of the polishing pad in 1% of H_2O_2 solution (Copied with permission [70]. Copyright 2016, Elsevier). (d) The number of carbon atoms removed at different sliding speeds during sliding (calculated by ReaxFF MD simulations) (Copied with permission [73]. Copyright 2021, Elsevier). (A colour version of this figure can be viewed online.)

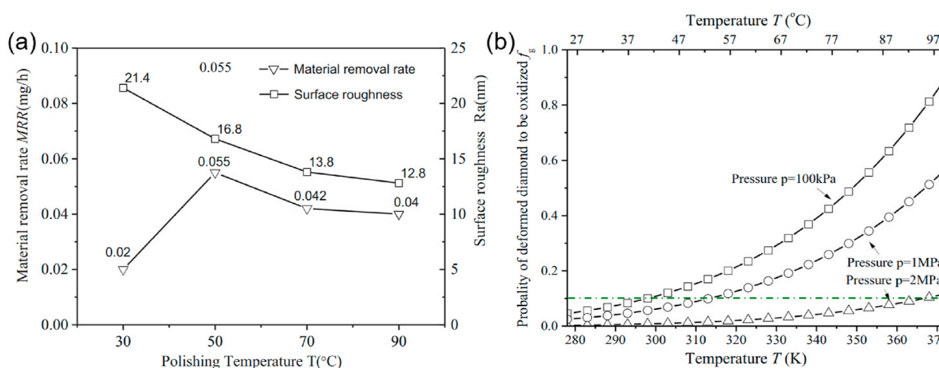

Fig. 10. (a) MRR and surface roughness of CVD diamond by performing CMP under different polishing temperature. (b) Probabilities of the oxidation reactions of diamond under different polishing temperature (Copied with permission [56]. Copyright 2018, Springer).

[66].

2.5. Evolution of surface topography during CMP

The main purpose of CMP is to achieve rapid large-area smooth surface processing with ultralow subsurface/surface damage. Understanding the surface morphology changes occurring during the polishing process is of direct significance in guiding the optimization of CMP processing technology [74]. Ideally, this understanding should be gained via observation of the topography evolution in-situ, to gauge the effects of all joint influencing parameters including the polishing duration. However, due to limitations of equipment, topography observation technology and surface cleaning technology, most studies have involved ex-situ topography characterisation. In general, higher load, speed, and oxidant concentration will result in a greater polishing rate, but not necessarily the best final surface topography of the polished surface. Excessive load and speed cause direct and serious damage to the subsurface structure and increase the difficulty of subsequent polishing. Moreover, although high oxidant concentration in the early stage is beneficial for accelerating the oxidation rate and improving the material removal efficiency, when most of the roughness has been removed, a high oxidant concentration will continue to destroy the freshly smoothened surface and prevent further reduction of surface roughness. For these reasons, choosing an appropriate processing parameter interval whilst systematically considering the coordination of various factors has become a key issue in the optimization of diamond polishing processes that involve both chemical and mechanical inputs.

Fig. 11 displays SEM and AFM images showing the typical evolution of surface topography during the polishing of NCD samples using a polishing slurry with silica nanoparticles. The as-grown PCD film shows crystal grains with size 100–250 nm. Compared to the pristine/as grown NCD (Fig. 11a), 4 h of CMP removes the majority of peaks and produces very smooth crystal plateaus lacking in voids or cracks and contamination (Fig. 11d). Measurements of the RMS roughness over 25 μm^2 after different polishing times show a drop in roughness from 18.3 nm to 4.5 nm after the first 2 h of polishing. However, the rate of surface roughness decrease reduced sharply in the subsequent 2 h, giving a final surface roughness after 4 h polishing of 1.7 nm. A similar trend was also observed in the polishing of an MCD surface, as shown in Fig. 2 [44]. In this case, the change in surface roughness experienced three stages with different roughness reduction rates during a 5 h polishing process. The higher polishing rate of MCD compared to the NCD case may be attributed to the larger grain size and greater height of the peaks and valleys of MCD. In the final stage, under the given process conditions, no further large changes occurred in the polishing rate or surface roughness of MCD and NCD [70,75,76].

3. Material removal mechanisms

In section 2, the review of factors affecting the MRR and surface roughness in diamond polishing processes demonstrates the great complexity of these processes and provides important clues regarding the different mechanisms that may govern material removal. Due to its ultra-high hardness and chemical inertness, it is difficult to mechanically abrade diamond using materials other than diamond itself, or to oxidize it under normal temperature and pressure conditions without the use of oxidizing agents. A large number of theoretical analyses and computational simulations have been conducted to try to understand the material removal mechanisms of diamond when both chemical and mechanical effects are involved in the polishing process. Such understanding is crucial for optimizing the polishing performance. In general, the material removal of diamond is dominated by the synergistic interaction of

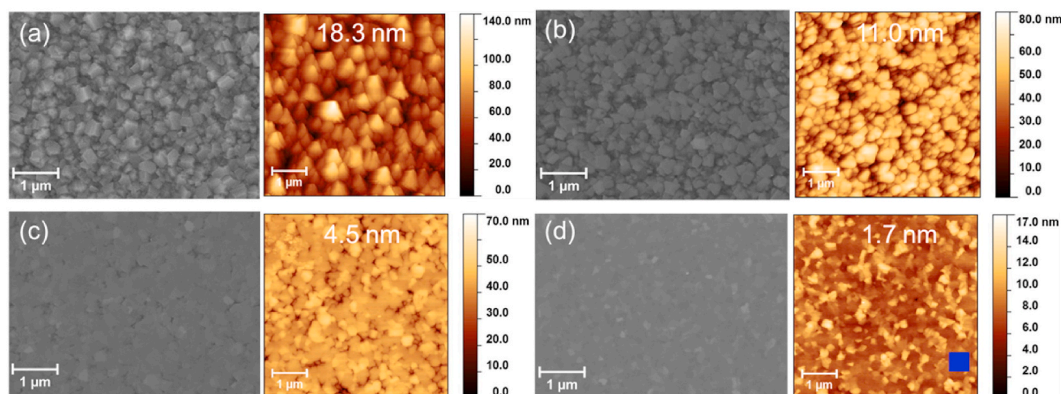

Fig. 11. SEM and AFM images of NCD films as-grown (a) and after 1 h (b), 2 h (c), and 4 h (d) CMP processes. The roughness values estimated over an area of 5 μm × 5 μm are displayed on the corresponding AFM images. (Copied under the terms of the Creative Commons license [69]).

mechanical stress/abrasion and chemical reaction. Such mechanochemical reactions refer to chemical reactions which are initiated or activated by external mechanical energy [77]. Under purely mechanical abrasive action, material removal can occur through mechanical deformation, scratching, crack formation and fracture under high contact pressure. However, mechanical interaction with diamond can also cause the diamond carbon structure itself to transform at the surface to a softer, more easily removed form of carbon that is also more readily oxidized. In addition, this same mechanical action can, through distortion of the C–C bonds, reduce the activation energy needed for a chemical reaction to take place at the diamond surface. Depending on the CMP slurry composition, chemical reactions can take place with oxide particles (SiO_2, Al_2O_3, CeO_2, etc.), leading to easier disruption of the C–C bonds of bulk diamond and material removal. Other mechanically-stimulated reactions can occur with oxidizing and reducing agents in the CMP slurry (e.g. H_2O_2, $Fe(NO_3)_3$, $KMnO_4$, $H_2C_2O_4$, etc.). These agents react readily with the diamond surface and generate a relatively soft layer containing C–O bonds on the diamond surface that can subsequently be removed by mechanical abrasive action, or lead to the formation of CO_2. Note here that the conversion of diamond to CO_2 is theoretically possible, but is only supported by simulations (see later section 3.1 and 3.2); there is no direct experimental evidence for CO_2 formation in previous studies.

As illustrated in Fig. 12a, the reaction activation barrier (E_a) of a C–C bond converting into a C–O or C=O bond (red line) is very high due to the strong covalent bonds in diamond. However, in the case of mechanochemical reaction, external mechanical energy can assist the diamond bonds to climb from their ground state (C) to a deformed diamond C* state (= C + δW, where δW mechanical work done for the chemical reaction) (Fig. 12a), significantly lowering the activation barrier (grey-dotted line, Fig. 12a). The reaction potential barrier E_1 between the C* and CO_2 states then becomes much lower than E_a. The reaction process in the presence of mechanical stimulation can be described as follows:

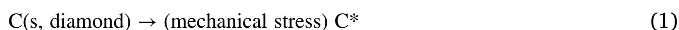

$$C(s, diamond) \rightarrow (mechanical\ stress)\ C^* \quad (1)$$

$$C^* + M \rightarrow CO_2 + N \quad (2)$$

where M and N are, respectively, oxidants and reaction products. Without shear stress or mechanical distortion, such reactions do not occur readily under room temperature and pressure conditions. Thus, synchronous and coupled mechanical and chemical interactions can be described as mechanically-activated, shear-induced or -facilitated chemical reactions, in this case a C–C bond converting to CO_2 over several energy peaks (activated states) [78]. The MRR in the polishing of diamond, in the case of mechanochemical reactions, can be quantified by the Arrhenius equation expressed below:

$$k = k_0 \cdot e^{-Ea/k_b\ T}, \quad (3)$$

where k is the reaction rate, k_0 is the pre-exponential factor, k_b is the Boltzmann constant (1.38 × 10^{-23} J/K), and T is temperature. The oxidation rate of diamond atoms with O_2 molecules at atmospheric temperature and pressure is approximately 3.7 × 10^{-28} g mm^{-2} (assuming E_a for the chemical reactions is 220 kJ/mol) [56,79].

As mentioned previously, the material removal processes involved in the mechanochemical polishing of diamond are complex; they depend greatly on the slurry composition and the magnitudes of parameters used in the polishing process and this makes it very challenging to elucidate the precise mechanisms involved. It is also likely that in many cases, if not all cases, more than one mechanism acts simultaneously and that these mechanisms are not mutually independent. In general however, three main routes leading to diamond material removal involving mechanochemistry can be distinguished:

1. Mechanically-stimulated chemical reaction of diamond with oxide particles in the polishing slurry, and subsequent removal of reaction products by the slurry. Here, this route is termed 'interfacial mechanochemical removal' and is exemplified by the conventional CMP process.
2. Chemical reaction (mechanically-stimulated) of diamond with strong oxidizing agents added to the polishing slurry, followed by abrasive removal of the layers formed, often aided by hard nanoparticles in the slurry. Here, this route is termed 'chemically-stimulated mechanical removal'.
3. Stress-induced transformation of diamond carbon, often in the presence of high carbon-solubility catalytic transition metals and their oxides, and subsequent removal of the softer, more readily oxidized, transformed material. Here, this route to material removal is referred to as 'mechanochemical transformation of diamond'.

3.1. Interfacial mechanochemical removal

As described above, mechanical energy can cause distortion of C–C bonds and promote their potential energy to a more activated state in which chemical reactions can occur more readily at ambient temperature and pressure, Fig. 12a. When relatively soft SiO_2 particles are used in the slurry during the CMP of diamond, purely mechanical removal of diamond is negligible; the mechanism of material removal is dominated by interfacial mechanically-stimulated chemical reactions.

To elucidate the mechanisms occurring, the reaction process taking place at the interface would ideally be monitored in-situ. However, this is not possible owing to the repeated action of multiple abrasives and the small contact areas involved, the rapidity with which carbon atoms are removed, and the limitations of characterization techniques. In addition, given that the interfacial chemical reaction and mechanical action are coupled, it is particularly difficult to characterize the atomic migration process and energy dissipation route at the nanoscale. However, theoretical analyses using MD simulation and density functional theory (DFT) [72,81–85], are able to provide insight into the atomistic details of the removal process with high temporal and spatial resolution. Previous studies have suggested that the chemical activity of the counter-surface significantly influences the mechanochemical reactions

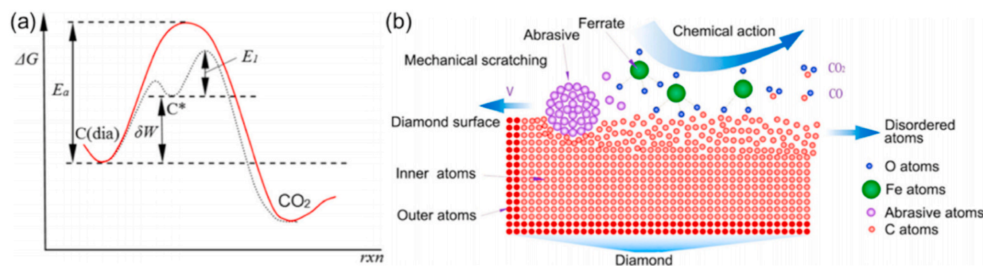

Fig. 12. (a) Simplified chemical coordinate of the C removal during the CMP of diamond (Copied with permission [56]. Copyright 2018, Springer). (b) Schematic diagram illustrating a diamond CMP process involving an oxidant (ferrate): carbon atoms are distorted and then removed by abrasive particles (Copied with permission [80]. Copyright 2020, Springer). (A colour version of this figure can be viewed online.)

occurring at the interface by altering the activation barrier of the bonding bridge formation [86,87]. Chemically active nanoparticles such as SiO_2, Al_2O_3, and CeO_2, have been widely used in the polishing slurry in the CMP of diamond [57,60]. Peguiron et al. duplicated the removal model of the diamond-silica sliding interface proposed by Thomas et al. by conducting DFT calculations of the atomic attrition taking place on (110) single crystalline diamond against silicon/silica [69,83]. The simulations demonstrated that a shear force applied in a system with diamond-silicon bonds at the interface would always lead to deformation of the silicon structure without breakage of the C–C bonds. However, a shear force applied at a silica-diamond sliding interface (Fig. 13a) was shown to lead to chemical activation and weakening of the C–C bonds (610 kJ/mol) in the underlying bulk diamond, resulting in mechanochemical breakage of the C–C bonds (Fig. 13b–g). The subsequent migration of the C–C–C zigzag unit marks the onset of diamond wear. The strong C–O bonds (1077 kJ/mol) formed at the interface under shear are crucial for the initial step in atomic attrition of the diamond surface against oxides. Werrell et al. hypothesized that crystalline Al_2O_3 or corundum should also be capable of promoting this mechanism [57]. Using Tight-Binding Quantum Chemical MD (TB-QCMD), Wang et al. discussed the influence of pressure on the friction-induced material removal at the sliding interface of an amorphous diamond surface [88]. A low friction coefficient of approximately 0.02 was predicted and no interfacial bonds were formed at the contacting interfaces when no tensile stress was present. However, interfacial C–C bonds were formed when tensile stress was applied, with the number of bonds increasing with increasing stress, leading to high friction (>1) and atomic attrition of the diamond surface. The atomic-level wear process was associated with the reaction coordinates of C–C bond dissociation caused by surface hydrogen transfer under high tensile stress.

Although DFT simulations can provide many local and short-lived results for chemical reactions with a high precision, the calculated reaction time and space-scale is restricted to a few picoseconds and a few hundreds of atoms due to the computational cost. Also, in such simulations, only the chemical reactions between nanoparticle abrasives and substrates can be considered; any chemical reactions resulting from oxidants in the polishing slurry, or the mechanical abrasion effect of components in this slurry, both of which fully participate in the interfacial reactions, are neglected. The ReaxFF MD method, developed by Duin et al. [89,90], is able to probe the reaction chemistry in larger-scale space and for a longer reaction time. However, the ReaxFF potential function was initially developed for hydrocarbons and silicates, and uses a general relationship between bond distance and bond order on the one hand, and between bond order and bond energy on the other hand, that leads to the proper formation and dissociation of chemical bonds. Because the ReaxFF potential function has not been developed specifically for diamond, the use of ReaxFF simulations is considered to be less accurate than DFT calculations, even though the simulated system is much larger than that of DFT. However, many results of ReaxFF, such as the oxidation of diamond to C–OH, O–C–O, and C═O, have been confirmed experimentally by X-ray photoelectron spectroscopy (XPS). Other results have not been verified, such as the formation of the "Si–O–C" bonding bridge and the generation of CO_2, due to the limitations of characterization techniques and experimental methods. The results of ReaxFF MD simulations provided by Shi et al. (Fig. 14a) revealed that diamond material removal by diamond nanoparticles in an OH radical environment can be attributed to mechanochemical interaction stimulated by external mechanical stress [85]. The applied mechanical stress can induce the decomposition of H_2O to passivate the diamond surface, forming C–H, C–O and C–OH bonds (Fig. 14b). The C–O/C–OH bonds activate adjacent C–C bonds for subsequent atomic removal in the form of CO or CO_2 (Fig. 14c). The combined effect of the C–O/C–OH bonds and mechanical shearing cause adjacent C–C bonds to be stretched and pulled away from the diamond substrate. The results of MD simulations by Yuan et al. indicated that increased pressure and sliding velocity result in a greater rate of carbon removal as a result of increased interfacial bonding. Moreover, even when a low pressure is applied, destabilization of the sp^3 structure at the surface can still occur after longer sliding distances, decreasing the activation energy for surface carbon removal [73].

To verify the mechanochemical reaction during the polishing of diamond, the chemical state and elemental composition of polished diamond substrates have been characterized using XPS analysis [56,68,69,91]. Fig. 15a shows that the C 1s peak (~285 eV) and O 1s peak (~531.0 eV) were the most dominant in the survey XPS spectra of an NCD surface polished using a slurry containing potassium ferrate oxidant. The presence of O on the diamond surface after the polishing process confirms that chemical reactions took place [69]. Fig. 15b displays high-resolution C 1s spectra of the as-grown and 4 h polished diamond thin films, which were deconvoluted into four chemical components: C–C (285.0 eV), C–H (285.5 eV), C–O (286.5 eV), and C═O (287.5 eV) [69,92,93]. It appears from this analysis that the chemical termination has not changed significantly as a result of the

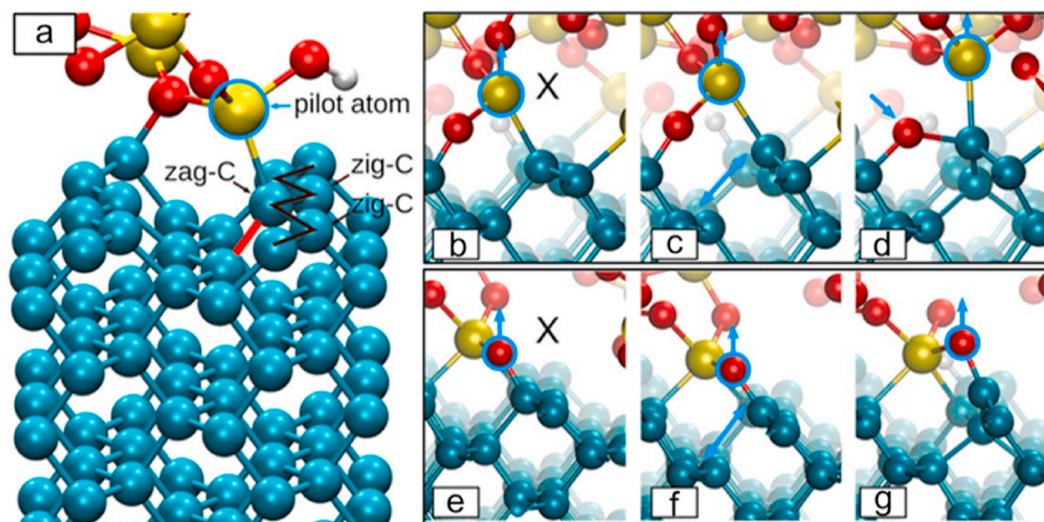

Fig. 13. DFT simulations of a C(110) substrate rubbed by silicon oxide. (a) The aromatic zigzag carbon chain (black) and a pilot atom (cyan circle) challenge the connected C–C bond (red) in the underlying bulk diamond. (b–g) Simulation steps for C–C bond breakage caused by mechanochemical reactions (Copied with permission [83]. Copyright 2016, Elsevier).

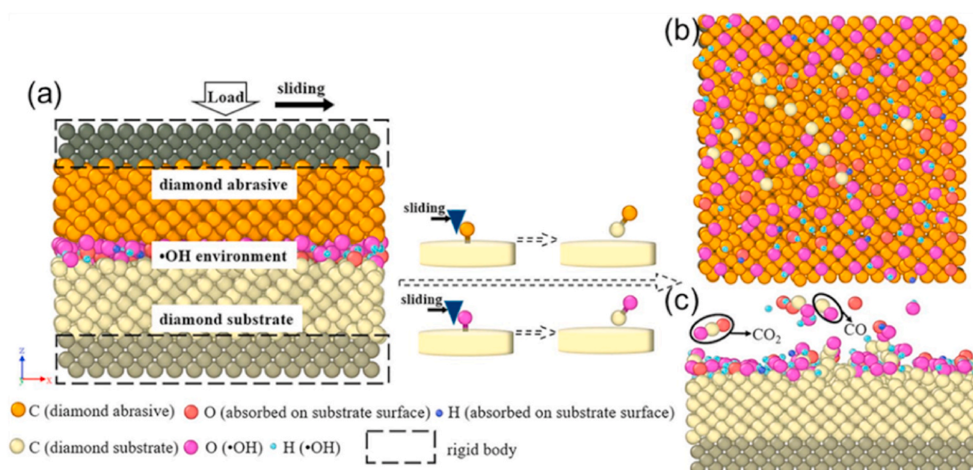

Fig. 14. (a) ReaxFF MD simulation model of diamond CMP in a radical OH environment. Structures of the abrasive (b) and the diamond substrate (c) after the CMP process (Copied with permission [85]. Copyright 2019, Elsevier).

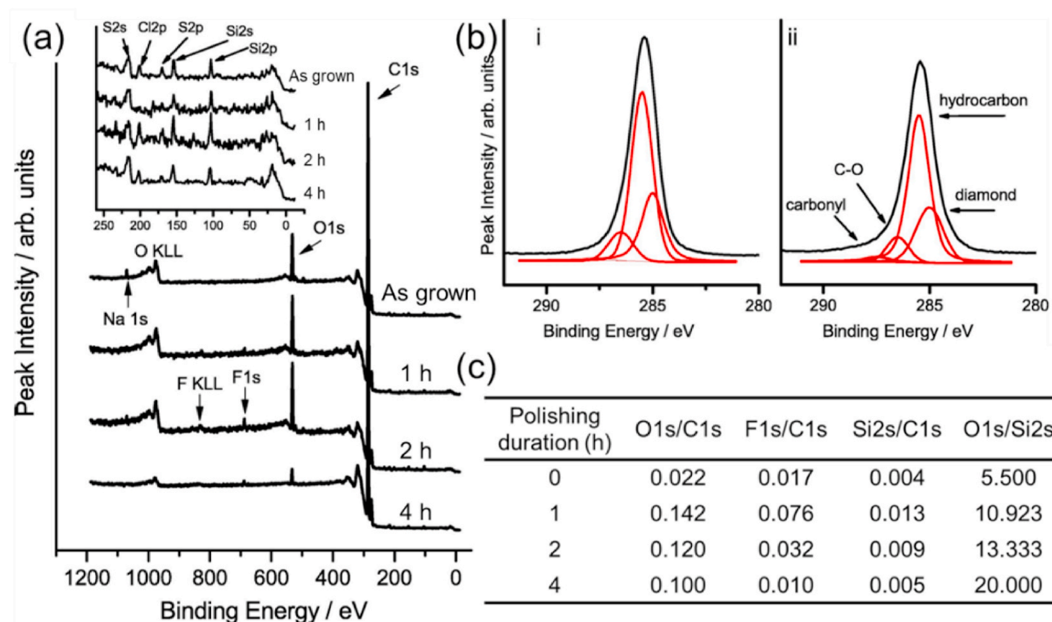

Polishing duration (h)	O1s/C1s	F1s/C1s	Si2s/C1s	O1s/Si2s
0	0.022	0.017	0.004	5.500
1	0.142	0.076	0.013	10.923
2	0.120	0.032	0.009	13.333
4	0.100	0.010	0.005	20.000

Fig. 15. (a) XPS Survey spectra of NCD substrates before and after CMP. Insert shows the XPS features at low binding energy. (b) C 1s spectra before (i) and after 4 h (ii) polishing, which were deconvoluted into diamond (C–C), hydrocarbon (C–H), ether (C–O), and carbonyl (C═O). (c) Elemental ratios of O 1s, F 1s, and Si 2s with respect to C 1s as a function of CMP duration. (Copied under the terms of the Creative Commons license [69]).

mechanochemical process, although there are subtle changes in the concentrations of the different carbon species. However, the mechanochemical process increased the oxygen content of the diamond surface, which was demonstrated by a significant increase in the ratio of O 1 s/C 1s after 1 h of polishing (Fig. 15c). The O 1s/Si 2s ratio increased with polishing time, suggesting that the oxygen signal in the XPS spectra originated from oxidized species other than silica.

The overall conclusion from the XPS analysis above is that the mechanochemical process always leads to general oxidation and increases in the C═O and C–OH content at the diamond surface. OH termination of the topmost surface could expedite the interfacial bonding connections of SiO_2 particles in the slurry solution (which are converted to $Si(OH)_4$ (silanol) in the presence of water) to the underlying diamond structure. The moving polishing pad provides a shear force on the silica particles that removes the particles and attached Si–OH molecules from the surface if the external mechanical energy is stronger than the weakened bond energy of the C–C bonds in the bulk diamond. An oxidized silica particle with OH terminated groups could also directly attach by itself, even if the diamond surface is not wet oxidized [69]. Subsequently, a Si–O–C bonding bridge is formed at the contacting interface between the silica nanoparticle and the diamond surface, and the C–C bond is broken with the help of tensile stress provided by the moving polishing pad.

3.2. Chemically-stimulated mechanical removal

Mechanochemical reactions occur at the uppermost layers of the surface, thus giving a relatively low MRR but a much smoother surface and lower surface damage compared to material removal induced solely by mechanical interactions (Fig. 2) [87,94]. In the interfacial mechanochemical removal discussed in section 3.1, the polishing pad provides the shear force for stimulation of the chemical reaction with oxide particles and removal of the reaction products. However, diamond can also readily be oxidized to CO and/or CO_2 by exposing it to an

environment that is oxygen-rich or contains strong oxidizing agents. The ensuing relatively soft oxide layer can subsequently be removed by the mechanical abrasion effect of hard nanoparticles (e.g. diamond or Al_2O_3) included in the slurry composition.

A process that has received much attention in recent years is to introduce strong oxidizing agents such as H_2O_2, KNO_3, $NaNO_3$, CrO_3, and K_2MnO_4 into the polishing slurry [64,65,70,95,96]. Molecular simulation studies reported by Kubota et al. [64,65,70] hypothesized that the uppermost part of the diamond surface first reacts with the oxidizing agents to form a chemically oxidized layer with relatively low hardness, which is then mechanically removed by abrasive action. In this way, the top layer of the diamond is quickly removed whilst material deeper in the structure is unaffected.

Yuan et al. explained the chemical reactions of diamond with selected oxidants on the basis of the Gibbs free energy ΔG [56]:

$$C(s, diamond) + O_2(g) \rightarrow CO_2(g),\ \Delta G^0 = -397.259\ kJ/mol \quad (4)$$

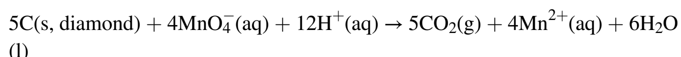

$$5C(s, diamond) + 4MnO_4^-(aq) + 12H^+(aq) \rightarrow 5CO_2(g) + 4Mn^{2+}(aq) + 6H_2O(l)$$

$$\Delta G^0 = -2532.669\ kJ/mol \quad (5)$$

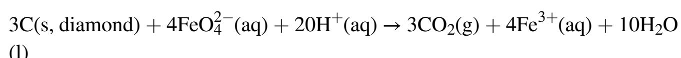

$$3C(s, diamond) + 4FeO_4^{2-}(aq) + 20H^+(aq) \rightarrow 3CO_2(g) + 4Fe^{3+}(aq) + 10H_2O(l)$$

$$\Delta G^0 = -2532.669\ kJ/mol \quad (6)$$

Thermodynamically, the three reactions above are spontaneous from left to right, however, without mechanical stimulation the reaction kinetics are unfavorable under ambient temperature and pressure conditions because of the high activation barrier. Clearly, the chemical reactivity of the surface atoms will be higher than that of atoms deeper within the bulk materials. However, during polishing these can also be more readily oxidized because of the mechanically-stimulated introduction of massive defects, such as lattice distortions, dislocations and cracks [97].

Fig. 12b schematically illustrates a diamond polishing process involving an oxidant (ferrate), in which carbon atoms are distorted and then removed by abrasive particles. There is a synergy between mechanical actions, which are driven by normal stress and shear stress, and chemical interactions with strong oxidants in the polishing slurry. Many investigations have shown that carbon atoms react readily with transition metals/high carbon soluble metals such as Ti, Fe, Ni, Mo, and Cr, either added as particles to the slurry or used as the polishing pad/plate. The reactions lead to the formation of carbides under elevated pressure or temperature conditions [45,98,99]. Surface polishing takes place through the chemically-activated transformation of sp^3 hybridized carbon atoms to a different hybridization structure, followed by diffusion into the carbon-soluble metals mentioned above, or the formation of CO_2 gas. Kubota et al. developed a polishing method using an iron plate in aqueous H_2O_2 solution to achieve an atomically-smooth diamond surface with a damage-free subsurface/surface [64,65,70]. The concentration of H_2O_2 solution in the polishing slurry was observed to play a crucial role in improving the MRR and optimizing the diamond surface roughness. The material removal process was described by Kubota et al. as following two steps: Firstly, the stable diamond structure undergoes chemical/oxidation reactions whereby the OH radicals react with the uppermost diamond layer. Subsequently, the weakened or softened layer, which was produced as a result of the chemical reactions on the diamond surface in the first step, is removed by the mechanical action of the polishing abrasive. However, material removal mechanisms assisted by chemical reactions between OH radicals (in polishing slurry) and a diamond surface are still far from understood. Some efforts have been conducted via MD simulations to "virtually observe" the atomic removal process occurring during the CMP of diamond in real time [67,85,100,101]. Guo et al. investigated the diamond CMP process using a silica abrasive in H_2O_2 solution by ReaxFF MD simulations. Fig. 16 shows carbon atoms removed in the form of CO, CO_2 and C chains (marked in black) in a series of similar removal steps. The above removal pathways of carbon atoms were explained by mechanical abrasive action occurring after oxidation reactions between diamond and H_2O_2 had resulted in a soft layer containing C–O, C–OH or C- bonds. Compared to a CMP process in pure H_2O, a greater number of carbon atoms were oxidized by H_2O_2 to form C–OH and C–O–C bonds and the predicted friction force was higher. It was claimed that the latter was due to stronger chemical reactions at the sliding interfaces, which presumably cause a higher interfacial shear strength. The results predicted that C atoms cannot be removed purely as a result of chemical reactions without mechanical abrasion, and that the removal rate is closely related to the pressure exerted by the nanoparticles in the slurry solution. A high load force and pressure facilitates the oxidation of the diamond surface, which leads to C atom removal, during the sliding process [101].

From the above, it can be concluded that the synergistic effect of chemical reaction with oxidizing agents and mechanical interaction can improve the removal rate without increasing the environmental temperature. The simulation results demonstrate that a strong oxidizing agent and a high mechanical stress imposed on the diamond surface can accelerate the carbon oxidation, simultaneously increasing the MMR. Mandal et al. characterised the chemical properties of NCD surfaces polished by an alkaline polishing slurry with the addition of three oxidants (H_2O_2, $Fe(NO_3)_3$, and $KMnO_4$) and two reductants ($C_2H_2O_4$ and $Na_2S_2O_3$) [68]. These additives accelerated the polishing process and resulted in a final polished diamond surface with less than 2 nm RMS roughness after 3 h of polishing. The survey XPS spectra shown in Fig. 17a suggest that there is little difference between the NCD surfaces polished using polishing slurries with the different redox agents. As an example (Fig. 17b), the C1s peak of the diamond surface polished by the polishing slurry with $C_2H_2O_4$ addition was deconvoluted into bulk and surface sp^3 C–C bonds (285 eV), graphitic carbon (284 eV), C–O/OH (286 eV), C=O (287.5 eV), and C(=O)OH (289 eV) groups. The

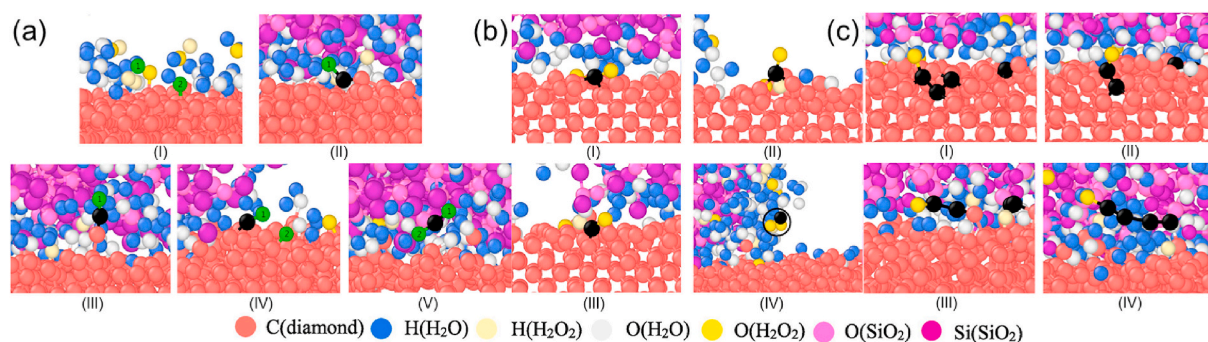

Fig. 16. Atomistic mechanisms of C(100) CMP in aqueous H_2O_2 solution. (a) C removal (black atoms) in the form of CO_2 (b), CO (c), and C chain (c) (Copied with permission [67]. Copyright 2019, Elsevier).

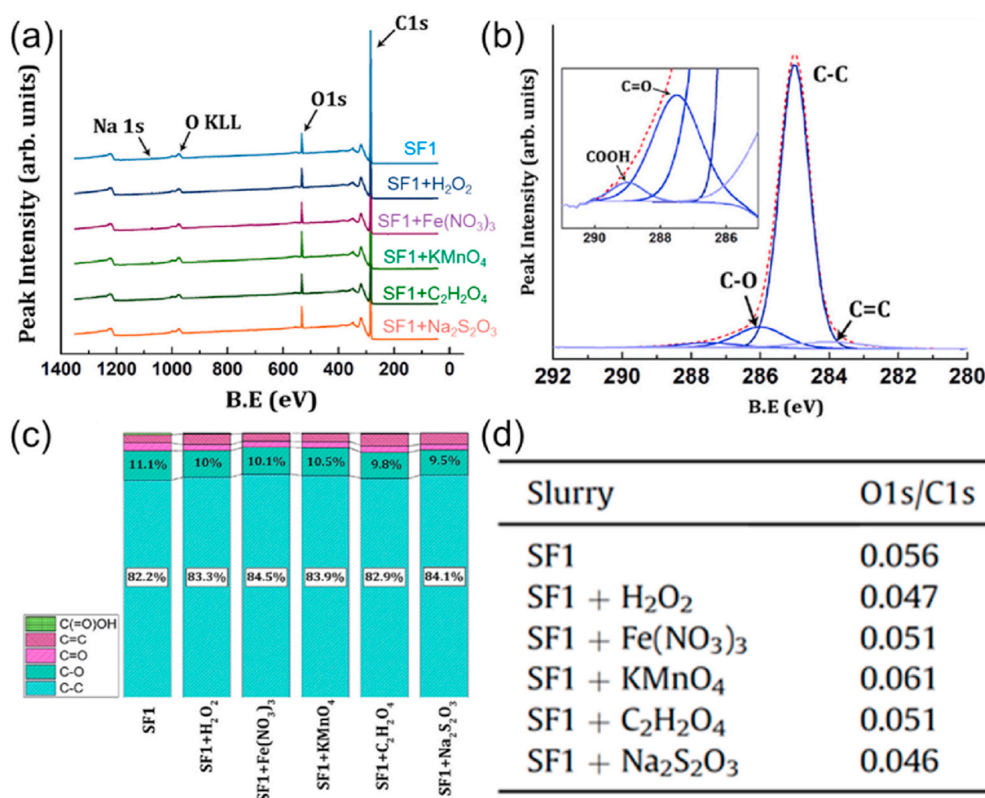

Fig. 17. (a) XPS survey spectra of NCD films that were polished with different redox agents. (b) Deconvolution of the C 1s peak obtained from the NCD surface polished by the slurry with $C_2H_2O_4$. (c) Components (C(=O)OH, C=C, C=O, C–O/OH, and C–C) of the C 1s peak in polished films. (d) Ratios of O 1 s/C 1s for 6 polished NCD samples (Copied with permission [68]. Copyright 2018, Elsevier).

constituent fractions and ratio of O 1 s/C 1s shows little difference for the six different kinds of oxidizing and reducing agents (Fig. 17c and d). This indicates that the addition of reductants does not increase the density of the oxygenated species on the surface but improves the polishing rate by promoting the chemical reaction rate for the same mechanical input.

3.3. *Mechanochemical transformation of diamond*

A third possible mechanism that can contribute to the removal of material from a diamond surface is stress-induced transformation of sp^3 hybridized (diamond) carbon, leading to a decrease in the surface hardness and an increase in the chemical activity [102,103]. Recent studies have found that subsurface lattice distortion, caused by mechanical stresses, is beneficial to the oxidation reactions of diamond atoms and that mechanical action can in this way effectively accelerate material removal [101]. The main types of carbon structure are diamond, amorphous carbon, graphite, and lons daleite (hexagonal diamond) [104]. Thermodynamically, graphite is stable at ambient temperature and pressure, whilst the other carbon lattice structures are metastable.

The reaction rate of the diamond structure transforming to graphite is slow under normal conditions and usually occurs only at high temperatures (>2000 K) [105]. However, as mentioned previously, the graphitization process can be catalysed by transition metals having a high carbon solubility. Such transition metals lower the energy barrier for transformation and enable graphitization to take place at relatively low temperatures of around 970 K [104,105]. The graphite can subsequently be removed by mechanical abrasion [104], in which case brittle fracture may play a large role [80]. It can also be readily oxidized because non-diamond carbon oxidizes faster than sp^3 hybridized (diamond) carbon due to a lower activation barrier (Fig. 12) and because of the faster diffusion rate and shorter diffusion path of carbon in graphite compared to diamond [104–106].

Diamond polishing experiments carried out by Zhang and Xu using an Fe-containing polishing wheel indicated that different mechanisms took place at different polishing speeds, presumably through a combination of differences in both temperature and mechanical stress (Fig. 18) [107]. A low polishing speed (less than 320 mm/s) promoted a removal mechanism based on micro-chipping and it was suggested that this was because the activation energy is insufficient to result in chemical reactions between diamond and the Fe-rich materials or to cause phase transformation of the diamond. At an intermediate polishing speed of 320–480 mm/s, the MRR was reported to be greatly improved due to the formation of Fe–C products with low wear resistance as a result of chemical reactions between diamond and Fe. At a polishing speed higher than 640 mm/s, it was hypothesized that the activation energy is decreased sufficiently that both chemical reactions between diamond and Fe and the conversion of diamond to graphite can occur [107]. It was shown by transmission electron microscopy (TEM) (Fig. 18e and f) that the diamond reacted initially with iron to form Fe_2C, and then underwent a diamond-graphite phase transformation during the mechanical abrasive action. Moreover, the surface/subsurface damage in the Fe_2C generation stage (with a thickness of 20–50 nm) was much less than in the diamond graphitization stage (with a thickness of ~1 μm) [107]. This means that, to optimize this particular polishing process, the reactions should be controlled in the carbide generation stage to ensure high removal efficiency while minimizing the subsurface damage.

There is also evidence that transition metal oxide particles can promote diamond transformation in polishing processes. Jin et al. investigated the role of α-Fe_2O_3 nanoparticles in the polishing processes of ultrahard nanotwinned diamond [108]. Using high-resolution TEM characterization, a large amorphous region containing Fe, O, and C was observed around the polishing area where Fe_2O_3 nanoparticles had

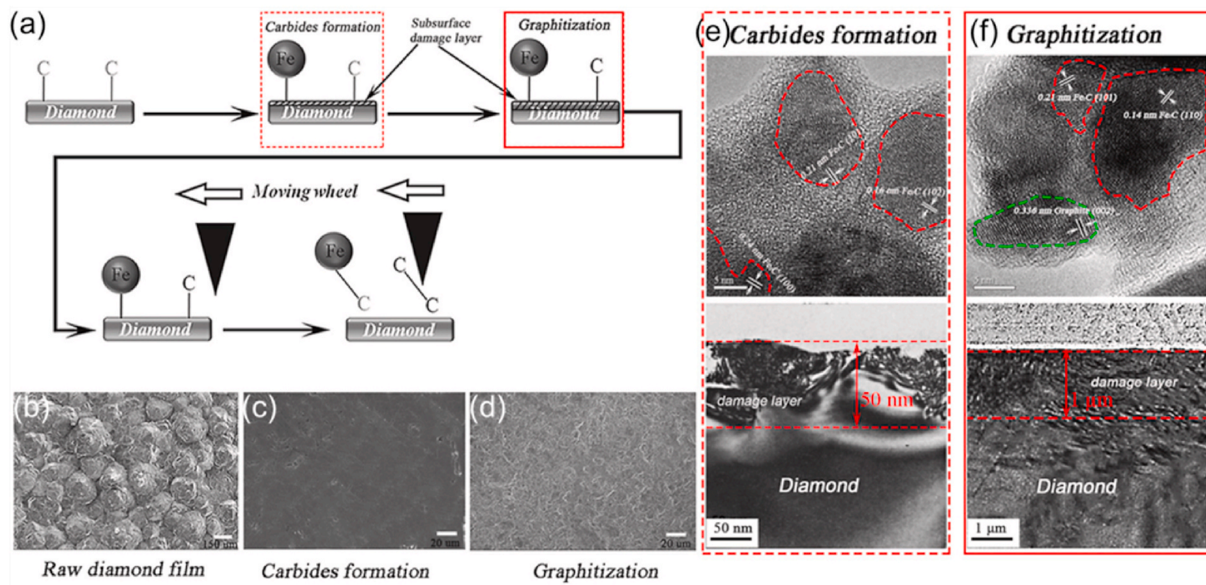

Fig. 18. (a) Schematic diagram of the material removal mechanism in diamond polishing with an Fe-containing wheel. SEM images of as-grown film (b), and polished films under the polishing speed of 480 mm/s (c) and 640 mm/s (d). Cross-sectional TEM images indicating the damaged subsurface after polishing with a speed of 480 mm/s (e) and 640 mm/s (f), with a fixed polishing distance of approximately 700 m (Copied with permission [107]. Copyright 2021, Elsevier).

penetrated the polished substrate. This observation indicates that a chemical reaction had taken place involving Fe, O, and C during polishing. It was speculated that α-Fe_2O_3 has high surface energy and that this catalyses the diamond amorphization.

4. Advanced diamond polishing methods involving a synergy between chemical and mechanical inputs

In broad terms, the process of smoothing a surface through the synergistic effect of chemical and mechanical interactions can be thought of as a combination of chemical reactions (etching, oxidation, diffusion, evaporation or their complex combinations) and abrasive polishing. Adding powerful oxidizing agents to the polishing slurry is an efficient way to introduce a chemical action at the sliding interfaces and improve the material removal efficiency. In addition, UV radiation and plasma radiation can act to powerfully promote oxidation reactions on diamond surfaces and polishing technologies using these radiation sources are under development to produce smooth diamond surfaces with low subsurface damage and high MRR.

4.1. UVAP

Watanabe et al. investigated a novel technique using UV light-induced photochemical reactions to assist the mechanochemical removal process of SCD in air at room temperature and pressure [109, 110]. In this process (Fig. 19a), the UV light is transmitted through a

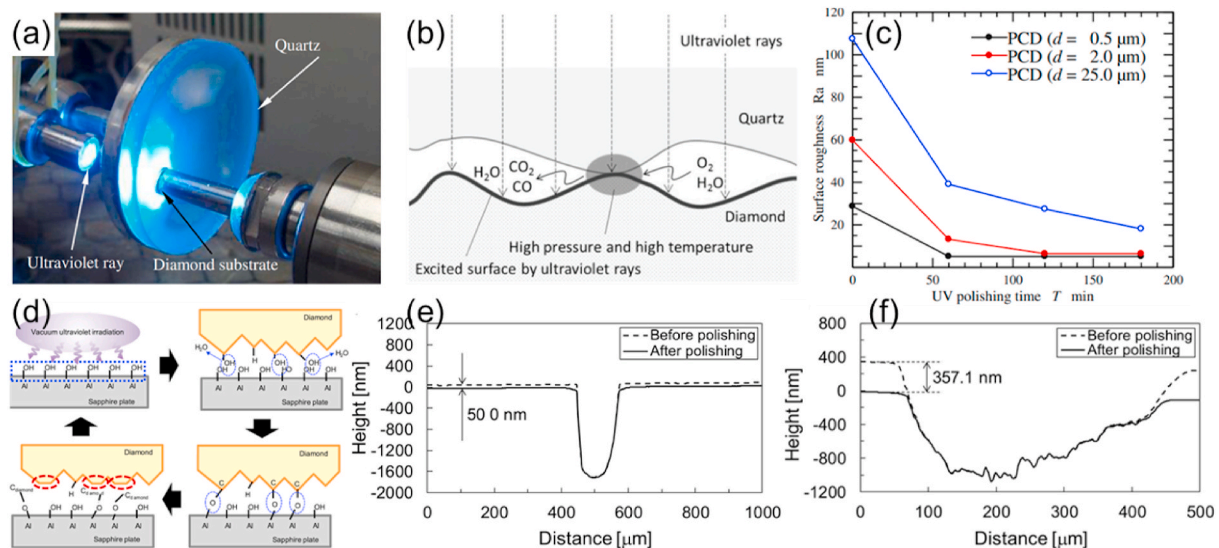

Fig. 19. (a) Image of home-built set-up for UVAP (Copied with permission [109]. Copyright 2013, Elsevier). (b) Principle of UV rays irradiation polishing (Copied under the terms of the Creative Commons license [112]). (c) The surface roughness of various PCD substrates with different grain sizes as a function of UVAP duration (Copied with permission [109]. Copyright 2013, Elsevier). (d) Schematic diagram of removal mechanism in VUVAP. The polishing rate was calculated by the difference in the depth of the marker track before and after UVAP (e) and VUVAP (f) (Copied with permission [111]. Copyright 2018, Elsevier). (A colour version of this figure can be viewed online.)

rotating quartz plate and irradiates the diamond sample directly whilst sliding against the plate. It was hypothesized that the carbon atoms on the diamond surface are excited by UV irradiation, leading to the generation of electron-hole pairs that rapidly react with O_2 and H_2O molecules in the surrounding air to form OH radicals and reactive oxygen species. These reactive species have a strong oxidizing effect on the carbon atoms of the SCD surface, forming CO or CO_2 gas as leaving products of the chemical reaction. At the same time, sp^3-hybridized carbon atoms are graphitized to sp^2 as a result of the surface temperature rise caused by the high sliding velocity and high pressure at the contact with the quartz plate (Fig. 19b). It was reported that the UV-irradiated method gave a MRR for the SCD substrate of 0.56 μm/h, three times higher than that without UV irradiation (0.14 μm/h) [109].

UVAP has also been successfully applied to PCD (MCD and NCD), producing a smooth surface with roughness of approximately 5.2 nm [109]. The grain size of the PCD strongly affects the polishing efficiency of UVAP. Fig. 19c displays the evolution of the R_a surface roughness with increasing polishing time on PCD surfaces with different grain sizes [109]. As the grain size decreased to less than 1 μm, the surface roughness (R_a) decreased from 30 nm to 5.2 nm within 1 h of polishing and with a comparatively high MRR of 2.0 μm/h. The UVAP rate could be further increased up to 6–7 μm/h by increasing the oxygen concentration of the chamber environment to approximately 82%. The authors attributed these results to the suppression of particle dropout and, because of the difference between the crystalline orientations of adjacent grains, uneven crystalline surfaces and a reduced contact area as the grain size decreases.

More recently, Kubota et al. have reported a further laboratory-scale development of the UV-assisted polishing method for SCD in vacuum conditions, which was termed vacuum ultraviolet assisted polishing (VUVAP) [111]. Compared to UVAP in ambient conditions, diamond surfaces planarized by VUVAP were shown to have a cleaner, hydrophobic surface with less organic contamination. A hypothesis for the removal mechanism involving reactions between the diamond and a sapphire (α-Al_2O_3) polishing plate is illustrated schematically in Fig. 19d. Firstly, the sapphire plate surface is fully oxidized by irradiation with 172 nm UV light and terminated with OH bonding groups. The terminated OH groups on the contacting surfaces then interact with each other, forming bonding bridges (C–O–Al) at the interfaces through a dehydration condensation reaction. Finally, the topmost C atoms are pulled away from the diamond surface as a result of breakage of the underlying C–C bonds induced by the combination of mechanical activation by relative motion and chemical reaction with the release of O_2 and H_2O molecules. In this way, a smooth diamond surface of 0.17 nm R_a is produced by the VUVAP process. The MRR can be calculated by measuring the difference in the depth of the wear track on the diamond surface, as shown in Fig. 19e and f. Based on the cross-sectional profiles of pristine and polished diamond surfaces, the MRR was calculated at 33.3 nm/h and 238.1 nm/h after 1.5 h of UVAP and VUVAP, respectively. It is important to note that the polishing set-up and conditions (e.g. downforce/contact pressure, speed, polishing plate) will greatly affect the results, so it is not possible to compare these absolute values directly with the results of other processes described in the literature. Nevertheless, the result that the VUVAP rate was found to be 7 times greater than the polishing rate using the same set-up in ambient conditions without VUV irradiation shows promise for this new technique.

4.2. PAP

Plasma irradiation is an effective method to create chemically reactive species; in the polishing of diamond it can be of benefit through the formation of a soft oxidized diamond layer, which can be more easily abraded, thus improving the polishing efficiency [113]. A PAP method, successfully used to polish GaN and SiC, was extended to the application of diamond polishing by Yamamura et al. [114–116] Using laboratory prototype PAP equipment (see Fig. 20a), a very smooth diamond surface of 0.13 nm R_a was achieved with a relatively high MRR of 2.1 μm/h. The PAP set-up used consisted of plasma generation and mechanical removal components. The plasma generating part was composed of an upper electrode and a rotating table made of aluminium alloy. As shown in Fig. 20a, the diamond-coated wafer was also rotated and in this way there was continuous alternation between the plasma irradiation treatment and the sliding material removal process. After chemically modifying the diamond surface by plasma-induced OH radicals, a 1 h polishing process improved the surface quality from 54 nm (pristine surface) to 0.46 nm (Fig. 20b and c). This could be further improved to

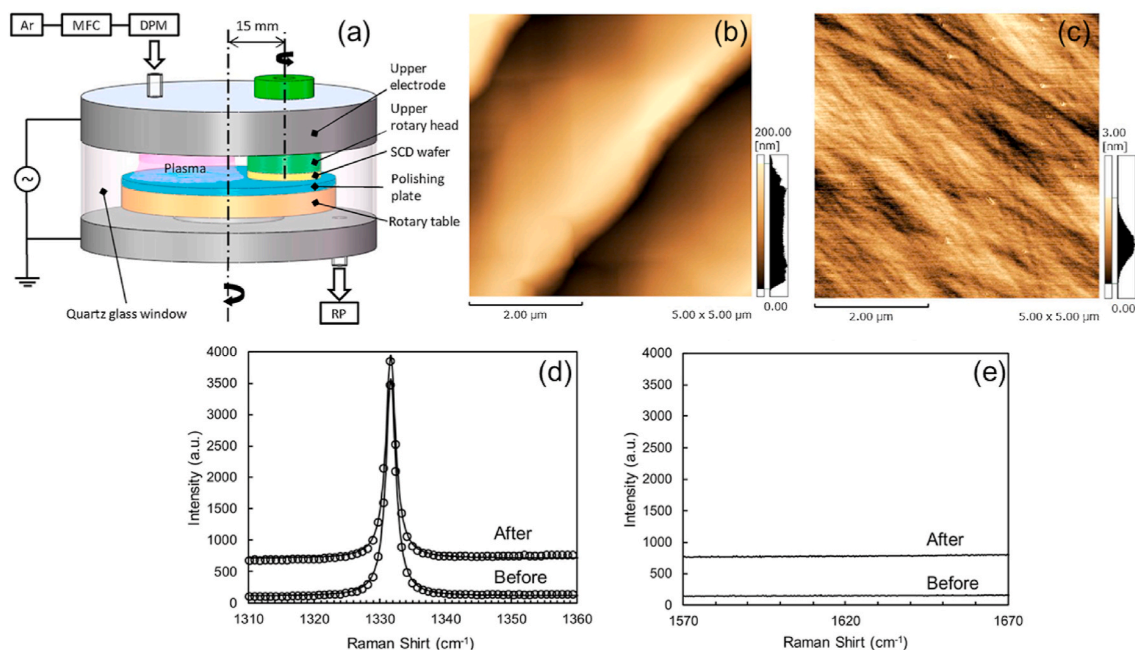

Fig. 20. (a) Schematic image of the experimental setups. A mass flow controller (MFC) was used to adjust the flow rate of Ar gas and a dew point meter (DPM) was employed to control the humidity. AFM images of SCD surface before (b) and after (c) PAP with a polishing pressure of 52.6 kPa and a polishing duration of 1 h. Micro-Raman spectra of C(100) before (d) and after (e) PAP (Copied with permission [114]. Copyright 2018, Elsevier).

0.13 nm using a sapphire plate instead of a quartz plate. Micro-Raman spectroscopy was used to evaluate the surface/subsurface structure of the polished diamond surface. The presence of carbon sp^3-bonding (diamond structure without blueshift at 1332 cm^{-1}) and no sp^2-bonding signal (graphite-like structure at 1580 cm^{-1}), as shown in Fig. 20d and e, indicates that no structural deformation or phase transformation (e.g., graphitization, amorphization) occurred during the PAP process and that the polished diamond surface was free of residual stress.

In the application of PAP to the polishing of semiconducting materials SiC, GaN, and sapphire, surface modification by, respectively, oxidation, fluorination, and O/OH termination are considered as possible mechanisms for PAP [115–117]. During the PAP of SiC and GaN, the uppermost layer of the hard lattice structure is softened and subsequently removed without destroying the subsurface structure. With sapphire, the OH termination or hydration of the uppermost surface by plasma treatment is thought to be responsible for the accelerated removal rate. The authors [115–117], suggest that the PAP mechanism for SCD is likely to coincide with the above description. The authors propose that, firstly, both the SCD and polishing plate surfaces are completely hydroxylated/OH-terminated by the plasma irradiation before the surfaces were brought in contact with each other. Subsequently, C–O–X (X refers to the Si atom from silicate glass or metal atoms from the polishing plate) bonding bridges are formed through dehydration reactions between two OH-terminated surfaces in the contact region. Finally, the relative motion between the SCD and polishing plate surfaces, which provides direct mechanical energy/shear stress, results in atom-by-atom C removal via the bonding bridge at the sliding interface without resulting in any graphitization or amorphization. Based on the above proposed removal mechanism, the oxidation reaction on the diamond surface induced by the plasma irradiation before the polishing process is likely to be the dominating factor in improving the MRR. By adding O_2 gas into the plasma irradiation process to enhance the hydroxylation reaction in the pre-treatment stage, it has been shown that the MRR of PAP for SCD can be improved to 13.3 μm/h [118].

In more recent work, Luo et al. used an inductively coupled plasma (ICP) modified silicon plate to perform CMP of SCD in atmospheric conditions in the absence of a slurry [119]. The authors claim, based on ICP discharge emission spectra and XPS analysis, that the ICP generates hydroxyl groups that modify the surface of the silicon plate, which subsequently aids attachment of these groups to the diamond surface. The ensuing chemical reaction at the OH-terminated silicon-diamond interface then leads to the formation of weak C–Si–O bonds that are easily removed by mechanical shearing, similar to the mechanism active when using silica slurry particles in an oxidizing slurry environment. The PAP method has not yet been applied successfully in the polishing of PCD surfaces, however, it is reasonable to expect similar results as with SCD.

Although the UVAP and PAP methods can significantly improve the polishing rate of diamond surfaces from several hundred nm/h to several μm/h through pre-oxidation treatments, these techniques are still in the laboratory research stage and the complexity of the required processing facilities currently inhibits widespread application. Moreover, the material removal mechanisms are still unclear and the existing computational simulations regarding the mechanochemical reactions between the polishing plate or fixed nanoparticles and UV and plasma irradiated diamond surfaces are still insufficient. Thus, much research is still needed before these techniques can be applied in an industrial setting. At the present time, CMP using polishing slurry remains the mainstream technology in ultra-high precision diamond surface processing, especially for the large scale and for ultra-low subsurface damage.

5. Perspective

A review of the literature on the polishing of diamond using different methods reveals that the material removal cannot be explained or predicted on the basis of simple independently-operating mechanical, chemical, or thermal actions at the polishing interfaces. General features of various polishing methods using mechanical and chemical inputs are listed in Table 1. MP and thermochemical polishing (TCP) are also listed for comparison purposes. However, it is not possible to make an exact comparison of cost in this review due to the great influence of the polishing scale, industrialization, and industry chain situation. Several polishing methods are still in the laboratory research stage and have not yet been implemented in an industrial environment or scale.

Mechanochemical reactions, occurring between the uppermost layers of the diamond substrates and nanoparticles in the polishing slurry, play pivotal roles, determining the polishing rate and the polished surface roughness. The mechanochemical reactions enable a set of reactants to undergo a process in which, energetically, the reaction climbs from the initial state (C–C) to the final state (C=O or C–O) over at least one intermediate step (via deformed or oxidized diamond) with a much lower reaction activation barrier. Although a great many studies have been carried out on diamond polishing processes involving chemical and mechanical synergies, research is still needed in the following areas:

5.1. Advanced methods

Based on the above summary, the material removal mechanism of diamond could be simply described as the oxidation- and/or deformation-induced material removal by atomic attrition of C atoms. Recently, several advanced methods (section 4) have been proposed that focus on how to enhance the oxidation reactions on the diamond surface before or during the polishing process. However, the technology is not yet mature: the material removal efficiency is still insufficient to meet the growing demand for ultra-precision diamond surfaces, and the complexity of the required processing equipment hampers the transfer and scale-up from the laboratory to large-scale industrial applications. Moreover, existing computational simulations of UVAP and PAP are still rather poor, requiring further investigation to improve understanding of the material removal mechanisms.

5.2. Advanced polishing slurry

Many studies are currently focused on changing the composition of the polishing slurry (oxidizers, transition metals/high carbon-soluble metal nanoparticles, pH, etc.) to accelerate the polishing rate and improve the surface quality. Since diamond is a chemically inert material, the development of polishing agents or nanoparticles with higher carbon reactivity is a promising way to further improve the diamond surface quality and provide a higher removal efficiency [120]. Although numerous studies concerning the effect of the polishing slurry recipe on the polishing efficiency and surface quality have been performed, both in a laboratory environment and in actual industrial processing environments, the empirical understanding gained is still limited. Especially for PCD films with surface heterogeneity in grain shape and grain chemistry, it is important to design the polishing slurry composition so as to find an appropriate balance between high MRR and surface uniformity.

Global environmental concerns require the use of “greener” technologies to reduce slurry consumption [121,122]. Other environmental impacts are present in the post-CMP cleaning which accompanies the CMP process, and in the removal of the particle and chemical contamination caused by the slurry. Thus, corrosion inhibitor -free slurry and abrasive-free slurry are currently being developed in order to enable a post-CMP cleaning step with easy removal of organic residues on the polished surfaces. The development of next-generation slurries remains a challenging issue in terms of the need to accommodate environmental requirements and at the same time introduce novel, more efficient and targeted slurry compositions that optimize the polishing performance.

Table 1
Overview of PCD polishing techniques. (MP and TCP are listed as comparisons).

Polishing method	MP	CMP	TCP	DFP	UVAP	PAP
Mechanism	Phase transformation of the diamond in the "soft" direction, micro-fracture	Oxidation (mechanochemical reactions), abrasion	Phase transformation, hot metal plate polishing, and thermo-diffusion etching	Phase transformation, mechanical abrasion, chemical reaction, and carbon solution induced by frictional heating	UV-assisted oxidation	Plasma-assisted oxidation
Environments	Air	Liquid (slurry solution), heater (>350 °C)	Controlled, heater (>700 °C)	Controlled	Air/Vacuum	Low pressure (2.3 kPa)
MRR	Tens of nm/h (traditional) [41], ~10 μm/h (rough chipping) [130], 200 μm/h (with ultrasonic vibration) [76]	16 nm/h (alkaline colloidal silica slurry solution) [69], 0.53, 0.76, 0.96, 1.39 μm/h (containing $KClO_3$, $KMnO_4$, H_2O_2 and $K_2S_2O_8$ regents) [45]	Several μm/h [131], >7 μm/h [132], ~9 μm/h [44]	Tens-hundreds of μm/h 12 μm/h (titanium plate) [133], 18, 35, 220 μm/h (cast iron, stainless steel 304, TiAl, FeNiCr alloy plate) [134]	For SCD: 0.56 μm/h [109], 0.24 μm/h (vacuum) [111] For PCD: 2.0 μm/h; 6–7 μm/h (adding O_2 gas) [109]	For SCD: 2.1 μm/h [114], 13.3 μm/h (adding O_2 gas) [118]
Reported roughness (R_a)	664 nm using cutoff length of 0.08 mm–0.8 mm (traditional) [44], ~1 μm (rough chipping) [130], ~0.5 μm over an area of 0.9 × 0.7 mm (with ultrasonic vibration) [76], 43.6 nm over an area of 20 μm × 20 μm [135]	95 nm using cutoff length of 0.08 mm–0.8 mm; 4.5 nm over an area of 3 μm × 3 μm [44], 2.8 nm over an area of 20 μm × 20 μm [135], 1.7 nm over an area of 5 μm × 5 μm [69], 1.8–2.7 nm over an area of 5 μm × 5 μm (with redox agents) [68]	25 nm [44], 6.22 ± 0.75 nm over an area of 50 μm × 50 μm [132]	3.6 μm (titanium plate) [133], 0.4 μm (cast iron, stainless steel 304, TiAl, FeNiCr alloy plate) [134]	For SCD: 0.21 nm over an area of 124 μm × 94 μm; 0.07 nm over an area of 1 μm × 1 μm [109], 0.13 nm over an area of 72 μm × 54 μm; 0.05 nm over an area of 1 μm × 1 μm (vacuum) [111] For PCD: 5.2 nm [109]	For SCD: 0.13 nm over an area of 1 μm × 1 μm [114], 0.4 nm over 5 μm × 5 μm (adding O_2 gas) [118]
Subsurface damage	High	Low	High	High	Low	Low
Maturity of process	Rough polishing used in industry	Most widely used in industry	Limited application in industry	Laboratory	Laboratory	Laboratory
Advantages	Fewer equipment requirements, low-cost, and flexibility	Ultra-smooth surface, ultra-low subsurface/surface damage, large polishing area, low-cost, and mature industrialization	High MRR	High MRR	High MRR, ultra-low subsurface/surface damage	High MRR, ultra-low subsurface/surface damage
Disadvantages	High damage (defects and lattice distortion) regarding both the diamond and the polishing wheel, low MRR, high crystal orientation anisotropy (very low polishing rate on "hard direction", such as (100) <110> and (111) <121>	Environmentally unfriendly, low MRR, and requires high temperature	Non-uniformity of the metal plate heating, high-cost, high subsurface/surface damage, and high complexity equipment (vacuum and high temperature)	High polishing speed and pressure, high subsurface/surface damage, mainly for rough polishing	The complexity of polishing facilities, high facilities cost, and unclear removal mechanism	The complexity of polishing facilities, high facilities cost, and unclear removal mechanism

5.3. Multi-scale material removal mechanisms

Up to now, most studies that have concerned material removal behaviors during the polishing of diamond can be divided into two types: fundamental research on atomic removal mechanisms using computational simulations (MD and DFT), and empirical polishing experiments under multi-asperity contact conditions. However, the gap between the experimental results and the simulation work, largely caused by algorithm and computing power limitations, still represents a great problem in properly elucidating the material removal mechanism for processes involving synergistic chemical and mechanical effects. Unfortunately, little experimental knowledge exists regarding the mechanochemical reactions at nano-asperity contacts between abrasive particles and crystalline diamond in aqueous solutions. Direct experimental evidence for the formation of the "Si–O–C" bonding bridge in interfacial mechanochemical reactions is still lacking. Unfortunately, wear debris produced in actual polishing conditions is expected to be lost with the polishing slurry, otherwise XPS inspection to determine the presence of "Si–O–C" bonds in the debris could be performed. Thus, appropriate wear test designs and methods for the collection of wear debris should be considered in the future.

Previous experimental studies have been largely focused on the mechanical properties (mechanical wear resistance, hardness, etc.) of carbon-based hard films, mainly diamond like carbon films. Such studies have concentrated primarily on the mechanical removal behavior in humid air or vacuum conditions for protective coating applications, rather than towards diamond polishing applications [123–125]. Exploring single-asperity scratching behavior in relation to the multi-asperity contact condition between a diamond substrate and abrasive particles in the slurry solution may help to build the connection between the simulation research results and actual experimental data [126,127]. There is also a need for a comprehensive study, from AFM-based single-asperity contact to multi-asperities contact, for actual polishing equipment [128,129]. In addition, current simulations focus on SCD. Atomistic simulations of the material removal process on PCD and amorphous diamond surfaces, in real mechanochemical diamond polishing environments and including the influences of atomic structure, grain size, grain boundary, and element doping, are required in order to

further the understanding of the polishing behaviors of diamond polishing processes.

Declaration of competing interest

The authors declare that they have no known competing financial interests or personal relationships that could have appeared to influence the work reported in this paper.

Acknowledgements

This work has been carried out at the Advanced Research Center for Nanolithography (ARCNL), a public-private partnership of the University of Amsterdam (UvA), the Vrije Universiteit Amsterdam (VU), the Netherlands Organisation for Scientific Research (NWO) and the semiconductor equipment manufacturer ASML. B.W. acknowledges funding from the NWO VENI grant No. VI.Veni.192.177.

References

[1] E. Fuentes-Fernandez, J. Alcantar-Peña, G. Lee, A. Boulom, H. Phan, B. Smith, et al., Synthesis and characterization of microcrystalline diamond to ultrananocrystalline diamond films via hot filament chemical vapor deposition for scaling to large area applications, Thin Solid Films 603 (2016) 62–68.
[2] O. Auciello, A.V. Sumant, Status review of the science and technology of ultrananocrystalline diamond (UNCD™) films and application to multifunctional devices, Diam. Relat. Mater. 19 (2010) 699–718.
[3] O.A. Shenderova, D.M. Gruen, Ultrananocrystalline Diamond: Synthesis, Properties and Applications, William Andrew Publishing, New York, 2006.
[4] C. Hébert, E. Scorsone, M. Mermoux, P. Bergonzo, Porous diamond with high electrochemical performance, Carbon 90 (2015) 102–109.
[5] P.W. May, Diamond thin films: a 21st-century material, Phil. Trans. Roy. Soc. Lond. 358 (2000) 473–495.
[6] G. Zhao, Z. Li, M. Hu, L. Li, N. He, M. Jamil, Fabrication and performance of CVD diamond cutting tool in micro milling of oxygen-free copper, Diam. Relat. Mater. 100 (2019), 107589.
[7] X. Cheng, Z. Wang, K. Nakamoto, K. Yamazaki, A study on the micro tooling for micro/nano milling, Int. J. Adv. Manuf. Technol. 53 (2011) 523–533.
[8] M. Frank, D. Breidt, R. Cremer, Nanocrystalline diamond coatings for machining, Vakuum Forsch. Praxis 19 (2007) 34–38.
[9] H.Y. Cheng, C.Y. Yang, L.C. Yang, K.C. Peng, C.T. Chia, S.J. Liu, et al., Effective thermal and mechanical properties of polycrystalline diamond films, J. Appl. Phys. 123 (2018), 165105.
[10] L. Booth, S.A. Catledge, D. Nolen, R.G. Thompson, Y.K. Vohra, Synthesis and characterization of multilayered diamond coatings for biomedical implants, Materials 4 (2011) 857–868.
[11] S. Kunuku, K.J. Sankaran, C.Y. Tsai, W.H. Chang, N.H. Tai, K.C. Leou, et al., Investigations on diamond nanostructuring of different morphologies by the reactive-ion etching process and their potential applications, ACS Appl. Mater. Interfaces 5 (2013) 7439–7449.
[12] Q. Yang, J. Zhao, Y. Huang, X. Zhu, W. Fu, C. Li, et al., A diamond made microchannel heat sink for high-density heat flux dissipation, Appl. Therm. Eng. 158 (2019), 113804.
[13] H. Umezawa, M. Nagase, Y. Kato, S.I. Shikata, High temperature application of diamond power device, Diam. Relat. Mater. 24 (2012) 201–205.
[14] A.M. Zaitsev, Optical Properties of Diamond: A Data Handbook, Springer Science & Business Media, Berlin, 2013.
[15] E. Ukraintsev, A. Kromka, W. Janssen, K. Haenen, D. Takeuchi, P. Bábor, et al., Electron emission from H-terminated diamond enhanced by polypyrrole grafting, Carbon 176 (2021) 642–649.
[16] V. Mortet, L. Drbohlavova, N. Lambert, A. Taylor, P. Ashcheulov, M. Davydova, et al., Conductivity of boron-doped diamond at high electrical field, Diam. Relat. Mater. 98 (2019), 107476.
[17] I. Kratochvílová, R. Škoda, J. Škarohlíd, P. Ashcheulov, A. Jäger, J. Racek, et al., Nanosized polycrystalline diamond cladding for surface protection of zirconium nuclear fuel tubes, J. Mater. Process. Technol. 214 (2014) 2600–2605.
[18] P. Ashcheulov, R. Škoda, J. Škarohlíd, A. Taylor, L. Fekete, F. Fendrych, et al., Thin polycrystalline diamond films protecting zirconium alloys surfaces: from technology to layer analysis and application in nuclear facilities, Appl. Surf. Sci. 359 (2015) 621–628.
[19] I. Kratochvilova, Polycrystalline diamond thin films for advanced applications, in: A. Silva, S. Carabineiro (Eds.), Advances in Carbon Nanostructures, InTechOpen, London, 2016, pp. 161–173.
[20] Eversole, WG., US Patent No. 3030188, April 17, 1962.
[21] M. Schwander, K. Partes, A review of diamond synthesis by CVD processes, Diam. Relat. Mater. 20 (2011) 1287–1301.
[22] M. Mertens, I.N. Lin, D. Manoharan, A. Moeinian, K. Bruehne, H.J. Fecht, Structural properties of highly conductive ultra-nanocrystalline diamond films grown by hot-filament CVD, AIP Adv. 7 (2017), 015312.
[23] H. Ye, C.Q. Sun, P. Hing, H. Xie, S. Zhang, J. Wei, Nucleation and growth dynamics of diamond films by microwave plasma-enhanced chemical vapor deposition (MPECVD), Surf. Coating. Technol. 123 (2000) 129–133.
[24] S. Matsumoto, M. Hino, T. Kobayashi, Synthesis of diamond films in a rf induction thermal plasma, Appl. Phys. Lett. 51 (1987) 737–739.
[25] D. Bhat, D. Johnson, A. Malshe, H. Naseem, W. Brown, L. Schaper, et al., A preliminary investigation of the effect of post-deposition polishing of diamond films on the machining behavior of diamond-coated cutting tools, Diam. Relat. Mater. 4 (1995) 921–929.
[26] R. Erz, W. Dötter, K. Jung, H. Ehrhardt, Preparation of smooth and nanocrystalline diamond films, Diam. Relat. Mater. 2 (1993) 449–453.
[27] Y. Tian, H. Liu, B.W. Sheldon, T.J. Webster, S. Yang, H. Yang, et al., Surface energy-mediated fibronectin adsorption and osteoblast responses on nanostructured diamond, J. Mater. Sci. Technol. 35 (2019) 817–823.
[28] H. Wang, J. Yang, F. Sun, Cutting performances of MCD, SMCD, NCD and MCD/NCD coated tools in high-speed milling of hot bending graphite molds, J. Mater. Process. Technol. 276 (2020), 116401.
[29] J.E. Butler, H. Windischmann, Developments in CVD-diamond synthesis during the past decade, MRS Bull. 23 (1998) 22–27.
[30] J.E. Butler, A.V. Sumant, The CVD of nanodiamond materials, Chem. Vap. Depos. 14 (2008) 145–160.
[31] O.A. Williams, Nanocrystalline diamond, Diamond Relat. Mater. 20 (2011) 621–640.
[32] S. Mandal, Nucleation of diamond films on heterogeneous substrates: a review, RSC Adv. 11 (2021) 10159–10182.
[33] D.M. Gruen, Nanocrystalline diamond films, Annu. Rev. Mater. Sci. 29 (1999) 211–259.
[34] T.A. Scott, The influence of microstructure on the mechanical properties of polycrystalline diamond: a literature review, Adv. Appl. Ceram. 117 (2018) 161–176.
[35] D. Miess, G. Rai, Fracture toughness and thermal resistance of polycrystalline diamond compacts, Mater. Sci. Eng. 209 (1996) 270–276.
[36] J.J. Alcantar-Peña, G. Lee, E.M. Fuentes-Fernandez, P. Gurman, M. Quevedo-Lopez, S. Sahoo, et al., Science and technology of diamond films grown on HfO_2 interface layer for transformational technologies, Diam. Relat. Mater. 69 (2016) 221–228.
[37] Z.W. Zhong, Recent developments and applications of chemical mechanical polishing, Int. J. Adv. Manuf. Technol. 109 (2020) 1419–1430.
[38] D. Zhao, X. Lu, Chemical mechanical polishing: theory and experiment, Friction 1 (2013) 306–326.
[39] H. Lee, D. Lee, H. Jeong, Mechanical aspects of the chemical mechanical polishing process: a review, Int. J. Precis. Eng. Manuf. 17 (2016) 525–536.
[40] B. Suryadevara, Advances in Chemical Mechanical Planarization (CMP), Woodhead Publishing, Cambridge, 2016.
[41] T. Schuelke, T.A. Grotjohn, Diamond polishing, Diamond Relat. Mater. 32 (2013) 17–26.
[42] A. Thornton, J. Wilks, The polishing of diamonds in the presence of oxidising agents, Diam. Res. 39 (1974) 39–42.
[43] M. Krishnan, J.W. Nalaskowski, L.M. Cook, Chemical mechanical planarization: slurry chemistry, materials, and mechanisms, Chem. Rev. 110 (2010) 178–204.
[44] H. Tsai, C. Ting, C. Chou, Evaluation research of polishing methods for large area diamond films produced by chemical vapor deposition, Diam. Relat. Mater. 16 (2007) 253–261.
[45] Y. Chen, L. Zhang, Polishing of Diamond Materials: Mechanisms, Modeling and Implementation, Springer Science & Business Media Berlin, 2013.
[46] X. Wang, X. Song, H. Wang, Y. Qiao, K. Larsson, F. Sun, Selective control of oxidation resistance of diamond by dopings, ACS Appl. Mater. Interfaces 12 (2020) 42302–42313.
[47] A. Gujrati, A. Sanner, S.R. Khanal, N. Moldovan, H. Zeng, L. Pastewka, et al., Comprehensive topography characterization of polycrystalline diamond coatings, Surf. Topogr-Metrol. 9 (2021), 014003.
[48] Y. Luo, L. Ma, L. Li, Y. Chen, K. Zhou, M. Yi, et al., Effect of bottom micro-crystalline diamond (MCD) layer and top nano-crystalline diamond (NCD) layer onto the tribological behavior of (MCD/NCD) bilayer film, Mater. Res. Express 7 (2020), 026412.
[49] O. Auciello, D.M. Aslam, Review on advances in microcrystalline, nanocrystalline and ultrananocrystalline diamond films-based micro/nano-electromechanical systems technologies, J. Mater. Sci. 56 (2021) 7171–7230.
[50] J.G. Buijnsters, M. Tsigkourakos, T. Hantschel, F.O. Gomes, T. Nuytten, P. Favia, et al., Effect of boron doping on the wear behavior of the growth and nucleation surfaces of micro-and nanocrystalline diamond films, ACS Appl. Mater. Interfaces 8 (2016) 26381–26391.
[51] A. Kumar Mallik, R. Bhar, S. Bysakh, An effort in planarising microwave plasma CVD grown polycrystalline diamond (PCD) coated 4in. Si wafers, Mater. Sci. Semicond. Process. 43 (2016) 1–7.
[52] H. Zeng, A.R. Konicek, N. Moldovan, F. Mangolini, T. Jacobs, I. Wylie, P. U. Arumugam, S. Siddiqui, R.W. Carpick, J.A. Carlisle, Boron-doped ultrananocrystalline diamond synthesized with an H-rich/Ar-lean gas system, Carbon 84 (2015) 103–117.
[53] N. Tatsumi, K. Harano, T. Ito, H. Sumiya, Polishing mechanism and surface damage analysis of type IIa single crystal diamond processed by mechanical and chemical polishing methods, Diam. Relat. Mater. 63 (2016) 80–85.
[54] E.L.H. Thomas, S. Mandal, E.B. Brousseau, O.A. Williams, Silica based polishing of {100} and {111} single crystal diamond, Sci. Technol. Adv. Mater. 15 (2014), 035013.

[55] B.S. El-Dasher, J.J. Gray, J.W. Tringe, J. Biener, A.V. Hamza, Crystallographic anisotropy of wear on a polycrystalline diamond surface, Appl. Phys. Lett. 88 (2006), 241915.
[56] Z. Yuan, P. Zheng, Q. Wen, Y. He, Chemical kinetics mechanism for chemical mechanical polishing diamond and its related hard-inert materials, Int. J. Adv. Manuf. Technol. 95 (2018) 1715–1727.
[57] J.M. Werrell, S. Mandal, E.L.H. Thomas, E.B. Brousseau, R. Lewis, P. Borri, et al., Effect of slurry composition on the chemical mechanical polishing of thin diamond films, Sci. Technol. Adv. Mater. 18 (2017) 654–663.
[58] S. Mandal, E.L. Thomas, J.M. Werrell, G.M. Klemencic, J. Ash, E.B. Brousseau, et al., Chemical mechanical polishing of nanocrystalline diamond, in: N. Yang (Ed.), Novel Aspects of Diamond: from Growth to Applications, Springer International Publishing, Cham, 2015, pp. 53–89.
[59] W. Choi, J. Abiade, S.M. Lee, R.K. Singh, Effects of slurry particles on silicon dioxide CMP, J. Electrochem. Soc. 151 (2004) G512–G522.
[60] H. Xu, J. Zang, P. Tian, Y. Yuan, Y. Wang, Y. Yu, et al., Surface conversion reaction and high efficient grinding of CVD diamond films by chemically mechanical polishing, Ceram. Int. 44 (2018) 21641–21647.
[61] J.G. Speight, Lange's Handbook of Chemistry, Mcgraw-hill, New York, 2005.
[62] S. Yuan, X. Guo, J. Huang, M. Lu, Z. Jin, R. Kang, et al., Sub-nanoscale polishing of single crystal diamond(100) and the chemical behavior of nanoparticles during the polishing process, Diam. Relat. Mater. 100 (2019), 107528.
[63] H. Kim, S. Hong, C. Shin, Y. Jin, D.H. Lim, J.Y. Kim, et al., Investigation of the pad-conditioning performance deterioration in the chemical mechanical polishing process, Wear 392–393 (2017) 93–98.
[64] A. Kubota, S. Nagae, S. Motoyama, M. Touge, Two-step polishing technique for single crystal diamond (100) substrate utilizing a chemical reaction with iron plate, Diam. Relat. Mater. 60 (2015) 75–80.
[65] A. Kubota, S. Nagae, M. Touge, Improvement of material removal rate of single-crystal diamond by polishing using H_2O_2 solution, Diamond Relat. Mater. 70 (2016) 39–45.
[66] H. Luo, K.M. Ajmal, W. Liu, K. Yamamura, H. Deng, Polishing and planarization of single crystal diamonds: state-of-the-art and perspectives, Int. J. Extreme Manuf. 3 (2021), 022003.
[67] X. Guo, S. Yuan, X. Wang, Z. Jin, R. Kang, Atomistic mechanisms of chemical mechanical polishing of diamond (1 0 0) in aqueous H_2O_2/pure H_2O: molecular dynamics simulations using reactive force field (ReaxFF), Comput. Mater. Sci. 157 (2019) 99–106.
[68] S. Mandal, E.L.H. Thomas, L. Gines, D. Morgan, J. Green, E.B. Brousseau, et al., Redox agent enhanced chemical mechanical polishing of thin film diamond, Carbon 130 (2018) 25–30.
[69] E.L.H. Thomas, G.W. Nelson, S. Mandal, J.S. Foord, O.A. Williams, Chemical mechanical polishing of thin film diamond, Carbon 68 (2014) 473–479.
[70] A. Kubota, S. Motoyama, M. Touge, Development of an ultra-finishing technique for single-crystal diamond substrate utilizing an iron tool in H_2O_2 solution, Diam. Relat. Mater. 64 (2016) 177–183.
[71] Z. Yuan, Y. He, Z. Jin, P. Zheng, Q. Li, Prediction of the interface temperature rise in tribochemical polishing of CVD diamond, Chin. J. Mech. Eng. 30 (2017) 310–320.
[72] S. Yuan, X. Guo, J. Huang, Y. Gou, Z. Jin, R. Kang, et al., Insight into the mechanism of low friction and wear during the chemical mechanical polishing process of diamond: a reactive molecular dynamics simulation, Tribol. Int. 148 (2020), 106308.
[73] S. Yuan, X. Guo, Q. Mao, J. Guo, A.C.T. van Duin, Z. Jin, et al., Effects of pressure and velocity on the interface friction behavior of diamond utilizing ReaxFF simulations, Int. J. Mech. Sci. 191 (2021), 106096.
[74] G.M. Klemencic, S. Mandal, J.M. Werrell, S.R. Giblin, O.A. Williams, Superconductivity in planarised nanocrystalline diamond films, Sci. Technol. Adv. Mater. 18 (2017) 239–244.
[75] C.Y. Cheng, H.Y. Tsai, C.H. Wu, P.Y. Liu, C.H. Hsieh, Y.Y. Chang, An oxidation enhanced mechanical polishing technique for CVD diamond films, Diam. Relat. Mater. 14 (2005) 622–625.
[76] V. Ralchenko, E. Ashkinazi, E. Zavedeev, A. Khomich, A. Bolshakov, S. Ryzhkov, et al., High-rate ultrasonic polishing of polycrystalline diamond films, Diam. Relat. Mater. 66 (2016) 171–176.
[77] Z. Liu, J. Gong, C. Xiao, P. Shi, S.H. Kim, L. Chen, et al., Temperature-dependent mechanochemical wear of silicon in water: the role of Si-OH surfacial groups, Langmuir 35 (2019) 7735–7743.
[78] C. Xiao, C. Deng, P. Zhang, L. Qian, S.H. Kim, Interplay between solution chemistry and mechanical activation in friction-induced material removal of silicon surface in aqueous solution, Tribol. Int. 148 (2020), 106319.
[79] F. Lu, J. Liu, G. Chen, W. Tang, C. Li, J. Song, et al., Oxidation behaviour of high quality freestanding diamond films by high power arcjet operating at gas recycling mode, Diam. Relat. Mater. 13 (2004) 533–538.
[80] F. Meng, Z. Zhang, P. Gao, T. Liu, Y. Boyjoo, D. Guo, Design of composite abrasives and substrate materials for chemical mechanical polishing applications, Appl. Nanosci. 10 (2020) 1379–1393.
[81] C. Huang, X. Peng, B. Yang, Y. Zhao, H. Xiang, X. Chen, et al., Molecular dynamics simulations for responses of nanotwinned diamond films under nanoindentation, Ceram. Int. 43 (2017) 16888–16894.
[82] W. Zong, X. Cheng, J. Zhang, Atomistic origins of material removal rate anisotropy in mechanical polishing of diamond crystal, Carbon 99 (2016) 186–194.
[83] A. Peguiron, G. Moras, M. Walter, H. Uetsuka, L. Pastewka, M. Moseler, Activation and mechanochemical breaking of C–C bonds initiate wear of diamond (110) surfaces in contact with silica, Carbon 98 (2016) 474–483.
[84] G. Zilibotti, S. Corni, M.C. Righi, Load-induced confinement activates diamond lubrication by water, Phys. Rev. Lett. 111 (2013), 146101.
[85] Z. Shi, Z. Jin, X. Guo, S. Yuan, J. Guo, Insights into the atomistic behavior in diamond chemical mechanical polishing with OH environment using ReaxFF molecular dynamics simulation, Comput. Mater. Sci. 166 (2019) 136–142.
[86] C. Xiao, C. Chen, H. Wang, L. Chen, L. Jiang, B. Yu, et al., Effect of counter-surface chemistry on defect-free material removal of monocrystalline silicon, Wear 426–427 (2019) 1233–1239.
[87] J. Guo, C. Xiao, J. Gao, G. Li, H. Wu, L. Chen, et al., Interplay between counter-surface chemistry and mechanical activation in mechanochemical removal of N-faced GaN surface in humid ambient, Tribol. Int. 159 (2021), 107004.
[88] Y. Wang, J. Xu, Y. Ootani, S. Bai, Y. Higuchi, N. Ozawa, et al., Tight-binding quantum chemical molecular dynamics study on the friction and wear processes of diamond-like carbon coatings: effect of tensile stress, ACS Appl. Mater. Interfaces 9 (2017) 34396–34404.
[89] K. Chenoweth, A.C. Van Duin, W.A. Goddard, ReaxFF reactive force field for molecular dynamics simulations of hydrocarbon oxidation, J. Phys. Chem. 112 (2008) 1040–1053.
[90] T.P. Senftle, S. Hong, M.M. Islam, S.B. Kylasa, Y. Zheng, Y.K. Shin, et al., The ReaxFF reactive force-field: development, applications and future directions, NPJ Comput. Mater. 2 (2016) 1–14.
[91] N. Dwivedi, R.J. Yeo, Z. Zhang, C. Dhand, S. Tripathy, C.S. Bhatia, Interface engineering and controlling the friction and wear of ultrathin carbon films: high sp^3 versus high sp^2 carbons, Adv. Funct. Mater. 26 (2016) 1526–1542.
[92] S. Ferro, M. Dal Colle, A. De Battisti, Chemical surface characterization of electrochemically and thermally oxidized boron-doped diamond film electrodes, Carbon 43 (2005) 1191–1203.
[93] J.I.B. Wilson, J. Walton, G. Beamson, Analysis of chemical vapour deposited diamond films by X-ray photoelectron spectroscopy, J. Electron. Spectrosc. Relat. Phenom. 121 (2001) 183–201.
[94] C. Xiao, X. Xin, X. He, H. Wang, L. Chen, S.H. Kim, et al., Surface structure dependence of mechanochemical etching: scanning probe-based nanolithography study on Si(100), Si(110), and Si(111), ACS Appl. Mater. Interfaces 11 (2019) 20583–20588.
[95] J. Haisma, F.J. van der Kruis, B.A. Spierings, J.M. Oomen, F.M. Fey, Damage-free tribochemical polishing of diamond at room temperature: a finishing technology, Precis. Eng. 14 (1992) 20–27.
[96] C. Wang, F. Zhang, T. Kuang, C. Chen, Chemical/mechanical polishing of diamond films assisted by molten mixture of $LiNO_3$ and KNO_3, Thin Solid Films 496 (2006) 698–702.
[97] S. Yuan, X. Guo, S. Zhang, C. Zhang, P. Li, Z. Jin, et al., Influence mechanism of defects on the subsurface damage and structural evolution of diamond in CMP process, Appl. Surf. Sci. 566 (2021), 150638.
[98] C. Artini, M. Muolo, A. Passerone, Diamond–metal interfaces in cutting tools: a review, J. Mater. Sci. 47 (2012) 3252–3264.
[99] X. Luo, J. Robin, S. Yu, Effect of temperature on graphite oxidation behavior, Nucl. Eng. Des. 227 (2004) 273–280.
[100] S. Yuan, X. Guo, M. Lu, Z. Jin, R. Kang, D. Guo, Diamond nanoscale surface processing and tribochemical wear mechanism, Diam. Relat. Mater. 94 (2019) 8–13.
[101] Z. Shi, Z. Jin, X. Guo, X. Shi, J. Guo, Interfacial friction properties in diamond polishing process and its molecular dynamic analysis, Diam. Relat. Mater. 100 (2019), 107546.
[102] S. Grillo, J. Field, The polishing of diamond, J. Phys. D Appl. Phys. 30 (1997) 202.
[103] L. Pastewka, S. Moser, P. Gumbsch, M. Moseler, Anisotropic mechanical amorphization drives wear in diamond, Nat. Mater. 10 (2011) 34–38.
[104] A. Malshe, B. Park, W. Brown, H. Naseem, A review of techniques for polishing and planarizing chemically vapor-deposited (CVD) diamond films and substrates, Diam. Relat. Mater. 8 (1999) 1198–1213.
[105] Y. Chen, L. Zhang, J. Arsecularatne, Polishing of polycrystalline diamond by the technique of dynamic friction. Part 2: material removal mechanism, Int. J. Mach. Tool Manufact. 47 (2007) 1615–1624.
[106] C. Lee, Effects of hydrogen and oxygen on the electrochemical corrosion and wear-corrosion behavior of diamond films deposited by hot filament chemical vapor deposition, Appl. Surf. Sci. 254 (2008) 4111–4117.
[107] M. Zhang, H. Xu, Controllability and mechanism investigation on the subsurface damage of CVD diamond film by Fe-containing vitrified bond wheel, Tribol. Int. 155 (2021), 106774.
[108] T. Jin, M. Ma, B. Li, Y. Gao, Q. Zhao, Z. Zhao, et al., Mechanical polishing of ultrahard nanotwinned diamond via transition into hard sp^2-sp^3 amorphous Carbon, Carbon 161 (2020) 1–6.
[109] J. Watanabe, M. Touge, T. Sakamoto, Ultraviolet-irradiated precision polishing of diamond and its related materials, Diam. Relat. Mater. 39 (2013) 14–19.
[110] S. Anan, M. Touge, A. Kubota, J. Watanabe, Study on ultra precision polishing of single crystal diamond substrates under ultraviolet irradiation, Key Eng. Mater. 407–408 (2009) 355–358.
[111] A. Kubota, T. Takita, Novel planarization method of single-crystal diamond using 172 nm vacuum-ultraviolet light, Precis. Eng. 54 (2018) 269–275.
[112] D. Ishimarua, M. Tougea, H. Mutaa, A. Kubota, T. Sakamoto, S. Sakamoto, Burr suppression using sharpened PCD cutting edge by ultraviolet-ray irradiation assisted polishing, Proc. CIRP 1 (2012) 184–189.
[113] M.L. Hicks, A.C. Pakpour-Tabrizi, R.B. Jackman, Polishing, preparation and patterning of diamond for device applications, Diamond Relat. Mater. 97 (2019), 107424.

[114] K. Yamamura, K. Emori, R. Sun, Y. Ohkubo, K. Endo, H. Yamada, et al., Damage-free highly efficient polishing of single-crystal diamond wafer by plasma-assisted polishing, CIRP Ann. 67 (2018) 353–356.
[115] K. Yamamura, T. Takiguchi, M. Ueda, H. Deng, A. Hattori, N. Zettsu, Plasma assisted polishing of single crystal SiC for obtaining atomically flat strain-free surface, CIRP Ann. 60 (2011) 571–574.
[116] H. Deng, K. Endo, K. Yamamura, Plasma-assisted polishing of gallium nitride to obtain a pit-free and atomically flat surface, CIRP Ann. 64 (2015) 531–534.
[117] C. Kageyama, K. Monna, H. Deng, K. Endo, K. Yamamura, Study on removal mechanism of sapphire in plasma assisted polishing, Adv. Mater. Res. 1136 (2016) 317–320.
[118] N. Liu, K. Sugawara, N. Yoshitaka, H. Yamada, D. Takeuchi, Y. Akabane, et al., Damage-free highly efficient plasma-assisted polishing of a 20-mm square large mosaic single crystal diamond substrate, Sci. Rep. 10 (2020) 1–7.
[119] H. Luo, K.M. Ajmal, W. Liu, K. Yamamura, H. Deng, Atomic-scale and damage-free polishing of single crystal diamond enhanced by atmospheric pressure inductively coupled plasma, Carbon 182 (2021) 175–184.
[120] Y. Lin, J. Lu, R. Tong, Q. Luo, X. Xu, Surface damage of single-crystal diamond (100) processed based on a sol-gel polishing tool, Diam. Relat. Mater. 83 (2018) 46–53.
[121] D. Lee, H. Lee, H. Jeong, Slurry components in metal chemical mechanical planarization (CMP) process: a review, Int. J. Precis. Eng. Manuf. 17 (2016) 1751–1762.
[122] L. Liu, Z. Zhang, B. Wu, W. Hu, F. Meng, Y. Li, A review: green chemical mechanical polishing for metals and brittle wafers, J. Phys. D Appl. Phys. 54 (2021), 373001.
[123] S. Miyake, S. Yamazaki, Nanoscratch properties of extremely thin diamond-like carbon films, Wear 305 (2013) 69–77.
[124] C. Charitidis, S. Logothetidis, M. Gioti, A comparative study of the nanoscratching behavior of amorphous carbon films grown under various deposition conditions, Surf. Coating. Technol. 125 (2000) 201–206.
[125] P. Shi, J. Sun, W. Yan, N. Zhou, J. Zhang, J. Zhang, et al., Roles of phase transition and surface property evolution in nanotribological behaviors of H-DLC: effects of thermal and UV irradiation treatments, Appl. Surf. Sci. 514 (2020), 145960.
[126] F.C. Hsia, F.M. Elam, D. Bonn, B. Weber, S.E. Franklin, Tracing single asperity wear in relation to macroscale friction during running-in, Tribol. Int. 162 (2021), 107108.
[127] Y. Liu, L. Chen, B. Jiang, Y. Liu, C. Xiao, J. Zhang, et al., Origin of low friction in hydrogenated diamond-like carbon films due to graphene nanoscroll formation depending on sliding mode: unidirection and reciprocation, Carbon 173 (2021) 696–704.
[128] J. Guo, J. Gong, P. Shi, C. Xiao, L. Jiang, L. Chen, L. Qian, Study on the polishing mechanism of pH-dependent tribochemical removal in CMP of CaF_2 crystal, Tribol. Int. 150 (2020), 106370.
[129] L. Chen, J. Wen, P. Zhang, B. Yu, C. Chen, T. Ma, X. Lu, S.H. Kim, L. Qian, Nanomanufacturing of silicon surface with a single atomic layer precision via mechanochemical reactions, Nat. Commun. 9 (2018) 1542.
[130] C. Tang, A. Neves, A. Fernandes, J. Gracio, N. Ali, A new elegant technique for polishing CVD diamond films, Diam. Relat. Mater. 12 (2003) 1411–1416.
[131] J. Weima, W. Fahrner, R. Job, Experimental investigation of the parameter dependency of the removal rate of thermochemically polished CVD diamond films, J. Solid State Electrochem. 5 (2001) 112–118.
[132] A. Zaitsev, G. Kosaca, B. Richarz, V. Raiko, R. Job, T. Fries, et al., Thermochemical polishing of CVD diamond films, Diam. Relat. Mater. 7 (1998) 1108–1117.
[133] S. Huang, L. Zhou, L.F. Xu, K. Jiao, A super-high speed polishing technique for CVD diamond films, Diam. Relat. Mater. 19 (2010) 1316–1323.
[134] Z. Yuan, Z. Jin, R. Kang, Q. Wen, Tribochemical polishing CVD diamond film with FeNiCr alloy polishing plate prepared by MA-HPS technique, Diamond Relat. Mater. 21 (2012) 50–57.
[135] C. Ollison, W. Brown, A. Malshe, H. Naseem, S. Ang, A comparison of mechanical lapping versus chemical-assisted mechanical polishing and planarization of chemical vapor deposited (CVD) diamond, Diam. Relat. Mater. 8 (1999) 1083–1090.